

Lepton flavor from a horizontal symmetry in a slice of AdS_5

Leandro Da Rold^{*}, Franco A. Gigena[◦], Jaime S. Guzmán Guerrero[†]

Centro Atómico Bariloche, Instituto Balseiro and CONICET

Av. Bustillo 9500, 8400, S. C. de Bariloche, Argentina

Abstract

We build a model of lepton flavor in a slice of AdS_5 . We add to the 5D SM fields a set of neutrino fields, as well as a horizontal $U(1)$ symmetry and a flavon field, all propagating in the bulk. The electroweak and $U(1)$ symmetries are spontaneously broken by a potential localized on the infrared boundary. We show that in a flavor anarchic scenario, by suitable choice of the 5D masses and the $U(1)$ charges, the masses of the SM leptons and the PMNS matrix can be naturally generated. The neutrino masses are Dirac like, with a normal ordered hierarchical spectrum, $\Delta m_{32}^2 \approx m_3^2$, $\Delta m_{21}^2 \approx m_2^2 \gg m_1^2$, and a suppressed θ_{13} mixing angle. We find configurations where the charged lepton mixing angles are suppressed by powers of the Cabibbo angle (λ_C) relative to vanilla anarchic partial compositeness, consequently reducing CP and lepton flavor violation. Specifically, the Wilson coefficient for the electron electromagnetic dipole moment exhibits λ_C^2 suppression, while those governing $\mu \rightarrow e\gamma$ and $\mu - e$ vector operators are suppressed by $\lambda_C^{3/2}$ compared to the anarchic scenario without $U(1)$ horizontal symmetry.

E-mails: ^{*} daroldl@ib.edu.ar, [◦] franco.gigena@ib.edu.ar, [†] jaime.guzman@ib.edu.ar

Contents

1	Introduction	3
2	A 5D model of leptons with horizontal U(1) symmetry	4
2.1	Texture of the neutrino mass matrix	6
3	Scalar sector of the 5D model and symmetry breaking	7
4	Spectrum and interactions of leptons	8
4.1	KK decomposition	8
4.2	Light leptons	11
4.3	Interactions with resonances in the mass basis	14
5	Lepton flavor violation	14
5.1	Low energy effective theory for lepton flavor violation	15
5.2	Estimates of the Wilson coefficients and comparison with APC	16
6	Numerical results	17
6.1	Lepton masses and mixing angles	18
6.2	Numerical results for the Wilson coefficients	19
7	Discussions and conclusions	21
A	KK decomposition of the scalar fields	23
A.1	Vacuum expectation values	24
A.2	Light states	25
B	Fermion matrix diagonalization	27

1 Introduction

The most widely considered solutions to the electroweak (EW) hierarchy problem that rely on symmetries introduce new physics (NP) at the TeV scale [1–4], with profound implications for flavor physics. For generic flavor structure of the NP sector the new states can mediate flavor transition processes with operators suppressed by the TeV scale, in severe contradiction with bounds from the experiments that require the scale of these operators to be of order 10^{2-5} TeV [5]. In most scenarios the hierarchy of masses and mixing angles of the Standard Model (SM) fermions is not explained.

There are several approaches to the flavor problem in these theories. In the framework of composite Higgs models, the partial compositeness mechanism, where the SM fermions have linear interactions with the composite sector, can generate the hierarchy of masses and mixings of the charged SM fermions [6–9]. An explanation of neutrino masses and mixing angles in anarchic partial compositeness (APC) usually requires new symmetries [10]. The chiral couplings suppressing the mass and mixing angles also suppress the flavor violating operators, realizing an approximate Glashow-Iliopoulos-Maiani (GIM) mechanism [11]. This framework has been thoroughly studied in warped extra dimensions [12], as well as in two site models [13] and in the context of the effective description of the strongly interacting light Higgs [14]. It has been shown that, despite the GIM-like suppression, for APC the masses of the resonances of the NP sector, m_* , have to be pushed above the TeV. In the quark sector the strongest constraint arises from Kaon physics, with $m_* \gtrsim 20$ TeV [15]. In the lepton sector the most severe constraint is the bound from the electromagnetic dipole moment (EDM) of the electron, that demands $m_*/g_* \gtrsim 200$ TeV, where g_* is the coupling between resonances [16].

On a different direction, abelian horizontal symmetries can also provide a rationale for the flavor structure of the leptons of the SM [17–19]. In the Froggatt-Nielsen (FN) framework, the Standard Model fermions and a new scalar flavon field Φ are charged under an additional $U(1)_{FN}$ symmetry [20–23]. Yukawa interactions arise from higher dimensional operators with powers of Φ that are determined by the charges of the fermions, p_f . When Φ acquires a vacuum expectation value, spontaneously breaking $U(1)_{FN}$, a flavor structure is generated with the effective Yukawa couplings being suppressed by $(\langle \Phi \rangle / \Lambda)^{|p_L - p_R|}$. FN provides a small parameter and an organizing principle for flavor, even with anarchic Yukawa couplings in the fundamental theory [24]. FN scenarios for the lepton flavor [25–39] have been studied in supersymmetric theories [40], in the presence of leptoquarks [41, 42], in the framework of modular symmetry [43] and in the context of elementary Axiflavor-Higgs unification [44]. Recently refs. [45, 46] identified viable charge assignments and studied lepton flavor violation (LFV). Several challenges remain, as the quest for the potential of the scalar fields, the need of many new heavy fermions and potential issues given the presence of an axion [47].

This work addresses the flavor structure of the leptonic sector in APC with a horizontal $U(1)$ symmetry ¹. We pursue two primary objectives. First, we aim to construct a natural model that simultaneously explains the charged lepton mass hierarchy, the neutrino mass-squared

¹See Ref. [48] for a model of quark flavor incorporating both mechanisms.

difference hierarchy, and the PMNS matrix, which includes two large mixing angles and a small one. It is highly challenging for APC or models with horizontal symmetries to individually account for these hierarchies. Second we seek to suppress LFV processes, thereby allowing the new physics scale to be lowered compared with vanilla APC (hereafter simply APC).

We construct a flavor-anarchic 5D model in a slice of AdS_5 , with the Standard Model fields propagating in the bulk. This setup is extended by a 5D $U(1)_{\text{FN}}$ gauge symmetry, a 5D flavon field and three 5D neutrino fields that are SM singlets. All the the fermions are charged under the new symmetry. Electroweak and $U(1)_{\text{FN}}$ breaking is achieved via an IR boundary potential, generating masses for the lepton 0-modes. The light neutrinos are of Dirac nature and, by appropriate choice of FN charges and 5D bulk masses, the observed hierarchies of masses and mixing angles are naturally reproduced, with $U_{\text{PMNS}} \simeq U_{\nu_L}$.

We study CP and lepton flavor violation (LFV) and compare the predictions with APC [49, 50]. As in that case, the largest contributions to these processes arise from vector and dipole operators, respectively generated at tree and one-loop level. We find that CP and LFV dipole operators are dominated by one-loop contributions with a heavy spin one resonance and with either a neutral or a charged Higgs. In the first case contributions are enhanced by the FN-charge squared, disfavoring large charges. We show that for suitable choices of 5D masses and charges the Wilson coefficient of dipole and vector operators are suppressed by powers of λ_C , compared with APC.

The paper is organized as follows: in sec. 2 we define a 5D model of leptonic flavor and determine a texture for the neutrino mass matrix. In sec. 3 we describe the scalar sector of the model, showing the conditions for spontaneous symmetry breaking and performing the Kaluza-Klein (KK) decomposition of the neutral fields. In sec. 4 we study the leptonic sector of the model, we perform the KK decomposition showing how to obtain the mass matrices of the light leptons and their interactions with the resonances. In sec. 5 we study LFV and in sec. 6 we show the numerical predictions. We present some discussions and conclusions in sec. 7. Some details regarding the KK decomposition of the scalar fields and the diagonalization of the fermion mass matrices are provided in Appendices A and B.

2 A 5D model of leptons with horizontal $U(1)$ symmetry

We consider a slice of AdS_5 and work in conformal coordinates, with the interval $ds^2 = a(z)^2(\eta_{\mu\nu}dx^\mu dx^\nu - dz^2)$, and the warp factor $a(z) = L/z$. The extra dimension is compactified on an interval with UV and IR boundaries at $z_0 \sim 10^{-15} \text{ TeV}^{-1}$ and $z_1 \sim \text{TeV}^{-1}$, respectively [51].

The Lagrangian of the 5D theory describing the flavor of the leptons is:

$$S_5 = \frac{1}{g_5^2} \int d^4x \int_{z_0}^{z_1} dz (\mathcal{L}_g + \mathcal{L}_f + \mathcal{L}_s + \mathcal{L}_y) \quad (1)$$

where the different terms correspond respectively to gauge, fermion and scalar sectors, as well as the Yukawa interactions. \mathcal{L}_g contains the kinetic term of the 5D gauge symmetry:

$SU(2)_L \times U(1)_Y \times U(1)_{FN}$. The boundary conditions (BCs) of the SM and FN gauge fields are chosen as $(++)$ and $(-+)$, respectively, leading to 0-modes that correspond to the 4D SM gauge fields only². We have factorized a coefficient $1/g_5^2$, with g_5 being the 5D expansion parameter³.

\mathcal{L}_f contains the kinetic and mass terms of the 5D fermions, with one field for each chiral lepton of the SM, plus a 5D neutrino field. We will denote the $SU(2)_L$ doublets by $L = (L^N, L^E)$ and the singlets by E and N . The 5D masses will be written as: $m_\Psi = c_\Psi/L$, with $\Psi = L, E, N$ and $c_\Psi \sim \mathcal{O}(1)$. The BCs ensure that every 5D field yields a 0-mode for each SM chiral fermion and a right-handed neutrino $N_R^{(0)}$ per generation. The charges of the leptons under the SM gauge group are the usual ones, whereas their charges under $U(1)_{FN}$ are denoted as $p_{L,E,N}$, see table 1. The FN charges of the leptons are not universal, we will elaborate on them on sec. 4

\mathcal{L}_s includes the 5D scalars H and Φ , with 0-modes identified as the 4D scalar Higgs and flavon fields, respectively:

$$\mathcal{L}_s = \sqrt{g} (|D_M H|^2 - m_H^2 |H|^2 + |D_M \Phi|^2 - m_\Phi^2 |\Phi|^2) , \quad (2)$$

where g is the determinant of the 5D metric and M labels the components in 5D: $(\mu, 5)$. We assume that the Higgs field is not charged under $U(1)_{FN}$, whereas Φ has charge $p_\Phi = 1/2$, as summarized in table 1. The BCs are taken as $(++)$ for both fields.

\mathcal{L}_y is given by:

$$\mathcal{L}_y = \sqrt{g} \left[x_N \bar{L} \tilde{H} N \left(\frac{\Phi^{(\dagger)}}{\Lambda_5} \right)^{\alpha_N} + x_E \bar{L} H E \left(\frac{\Phi^{(\dagger)}}{\Lambda_5} \right)^{\alpha_E} \right] + \text{h.c.} , \quad (3)$$

$$\alpha_N = 2|p_L - p_N| , \quad \alpha_E = 2|p_L - p_E| , \quad (4)$$

where generation indices are understood for the fields as well as for the couplings and the exponents $\alpha_{N,E}$. The choice between Φ and Φ^\dagger in the interactions is determined by the sign of $(p_L - p_N)$ and $(p_L - p_E)$, ensuring that the Yukawa couplings remain invariant under the $U(1)_{FN}$ symmetry. Λ_5 denotes the cut-off scale of the 5D theory, with $\Lambda_5 \sim 24\pi^3/g_5^2$. The couplings $x_{N,E}$ are dimensionless $\mathcal{O}(1)$ parameters, assumed to be anarchic in flavor space. Upon canonical normalization of the fields, the 5D Yukawa couplings take the form $x_{N,E} g_5$. As is typical in FN models, replacing Φ with its vacuum expectation value (vev) induces effective 5D Yukawa couplings with a non-trivial flavor structure, governed by the FN charges: $x_{N,E} (v_\Phi/\Lambda_5)^{2|p_L - p_{N,E}|}$.

The UV and IR boundaries host quadratic and quartic potentials in the scalar fields, respectively:

$$S_{bd} = \int d^4x [a^4(z_0) V_0 - a^4(z_1) V_1] , \quad (5)$$

$$V_0 = (m_{0H}^2 |H|^2 + m_{0\Phi}^2 |\Phi|^2)|_{z_0} , \quad (6)$$

$$V_1 = (m_{1H}^2 |H|^2 + m_{1\Phi}^2 |\Phi|^2 + \lambda_{1H} |H|^4 + \lambda_{1\Phi} |\Phi|^4 + \lambda_{1\Phi H} |\Phi|^2 |H|^2)|_{z_1} , \quad (7)$$

the subscripts 0 and 1 refer to the UV and IR boundaries at z_0 and z_1 , respectively.

²(+) and ⁽⁻⁾ denote Neumann and Dirichlet BCs, respectively, the first sign is for the UV BC and the second one for the IR BC.

³While we use a single common coupling g_5 for brevity, distinct couplings may be assigned to each Lagrangian term. This is required, for example, to match the 4D gauge couplings.

field	$SU(2)_L$	$U(1)_Y$	$U(1)_{FN}$
H	2	1/2	0
Φ	1	0	1/2
L	2	1/2	p_L
E	1	-1	p_E
N	1	0	p_N

Table 1: Representations of the the 5D leptons and scalar fields.

2.1 Texture of the neutrino mass matrix

We will consider Dirac-type neutrinos, with normal ordering and a PMNS matrix dominated by the neutrino sector, meaning that the mixing angles of the Left-handed charged leptons are much smaller than those of the neutral ones. This feature enables the suppression LFV processes. The masses and mixing angles of the SM neutrinos are determined with high accuracy by the mass matrix of the would be 0-modes obtained after dimensional reduction, neglecting the effect of mixing with the KK states.

We find it useful to express the hierarchy of masses and mixing angles in powers of λ_C . Although the power of λ_C featuring angles and ratios of masses is not an exact number, and it depends on the renormalization scale, we will consider approximate values valid at a few TeV scale [52]. For the hierarchical normal order of neutrino masses we will use:

$$m_{\nu 1} \sim \lambda_C^2 m_{\nu 3}, \quad m_{\nu 2} \sim \lambda_C m_{\nu 3}. \quad (8)$$

The PMNS matrix has a non-hierarchical structure, except for $\theta_{13} \simeq 0.15 \sim \lambda_C$, whereas $\theta_{12} \sim \theta_{23} \sim \mathcal{O}(1)$. Since we are interested in the limit: $U_{PMNS} \simeq U_{\nu_L}$, we will work with [53]

$$U_{\nu_L} \sim \begin{pmatrix} 1 & 1 & \lambda_C \\ 1 & 1 & 1 \\ 1 & 1 & 1 \end{pmatrix}. \quad (9)$$

The following neutrino mass matrix satisfies the previous conditions:

$$M_\nu \sim m_{\nu 3} \begin{pmatrix} \lambda_C^2 & \lambda_C & \lambda_C \\ \lambda_C^2 & \lambda_C & 1 \\ \lambda_C^2 & \lambda_C & 1 \end{pmatrix}. \quad (10)$$

For the hierarchy of charged lepton masses we consider the following expressions:

$$m_e \sim \lambda_C^5 m_\tau, \quad m_\mu \sim \lambda_C^2 m_\tau. \quad (11)$$

In sec. 4 we will show configurations of 5D masses and FN charges that in the 0-mode approximation lead to Eqs. (10) and (11), as well as small mixing angles in the charged sector.

3 Scalar sector of the 5D model and symmetry breaking

Let us now consider the scalar sector of the model. We focus on the radial mode of the scalars, describing the vevs and the first KK state ⁴. We present the results that are relevant for the theory of leptonic flavor. The details of the calculations of the potential, as well as of the KK decomposition, are given in Ap. A.

The potential localized on the IR boundary, V_1 , triggers the spontaneous breaking of the EW and FN symmetries, preserving the electromagnetic symmetry. The vevs of the scalar fields, $\langle H^t \rangle = (0, v_H(z))$ and $\langle \Phi \rangle = v_\Phi(z)$, can be written as [55]:

$$v_\chi(z) = v_{\chi 4} \frac{g_5}{\sqrt{L}} \frac{z_1}{L} \left(\frac{z}{z_1} \right)^{2+\beta_\chi} F(2+2\beta_\chi) , \quad \chi = H, \Phi , \quad (12)$$

where $\beta_\chi = \sqrt{4 + m_\chi^2 L^2}$ and the function $F(x)$ is defined by:

$$F(x) = \left[\frac{x}{1 - (z_0/z_1)^x} \right]^{1/2} . \quad (13)$$

Notice that this function, given the large hierarchy between z_0 and z_1 , can have an exponential dependence on its argument, with $F(x) \rightarrow \sqrt{x} (z_0/z_1)^{x/2}$ for $x < 0$, $F(x) \rightarrow \sqrt{x}$ for $x > 0$ and $F(x) \rightarrow [\log(z_1/z_0)]^{-1/2}$ for $x \rightarrow 0$. ⁵

The 4D vevs are obtained as the integrals of the 5D ones along the extra-dimension:

$$v_{\chi 4}^2 = \frac{1}{g_5^2} \int dz a(z)^3 v_\chi(z)^2 , \quad \chi = H, \Phi . \quad (14)$$

Since the scalar fields are mixed by $\lambda_{1\Phi H}$ in V_1 , we perform the following KK decomposition:

$$h(x^\mu, z) = \sum_n s^{(n)}(x^\mu) f_n^h(z) , \quad \phi(x^\mu, z) = \sum_n s^{(n)}(x^\mu) f_n^\phi(z) , \quad (15)$$

where $s^n(x^\mu)$ are the 4D KK scalar modes, with projections on the 5D fields $h(x^\mu, z)$ and $\phi(x^\mu, z)$ given by the KK profiles $f_n^h(z)$ and $f_n^\phi(z)$, respectively.

We are interested in a region of the parameter space able to generate a light state $s^{(1)}$ that could be identified with the Higgs, with states $s^{(n>1)}$ heavy enough to evade the bounds from searches of scalar resonances. Besides, since the Higgs couplings have been measured in agreement with the SM, the KK wave function of the light state must be dominated by the projection f_1^h , with only a small projection f_1^ϕ . A small coupling $\lambda_{1\Phi H}$ can avoid large mixing between the scalars. In Fig. 1 we show the KK wave functions of the first and second modes for a point of the parameter space with KK masses $m_1 \simeq 125$ GeV and $m_2 \simeq 544$ GeV. The point

⁴The angular mode of Φ can lead to a 4D axion, that can obtain a mass from the KK gluons [54], the analysis of the angular modes is beyond the scope of this paper.

⁵ F can be related with the degree of compositeness of two-site theories.

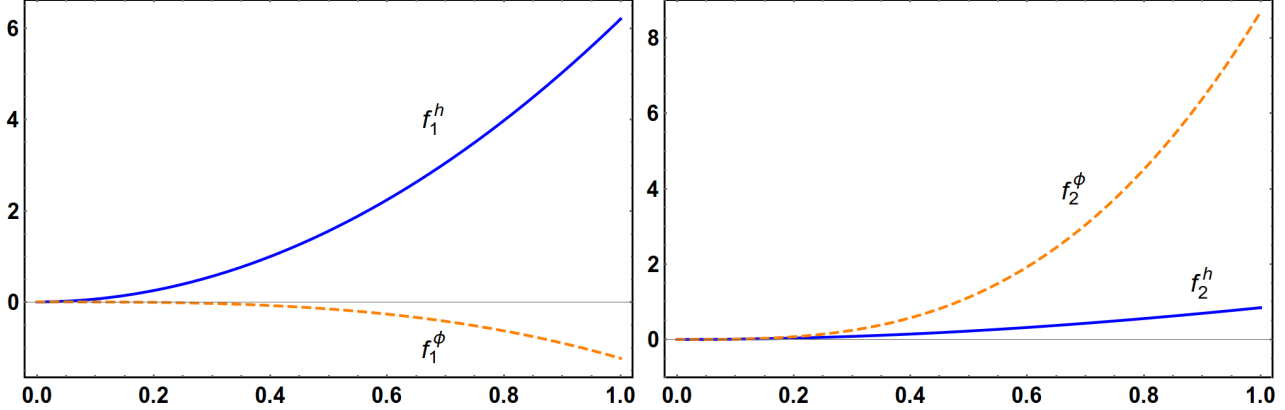


Figure 1: KK wave functions of the first and second scalar modes: $s^{(1)}$ and $s^{(2)}$, respectively.

of the parameter space of the 5D theory is given by: $\beta_H = 0$, $\beta_\Phi = 1$, $\lambda_{1H} = \lambda_{1\Phi} = \lambda_{1\Phi H} = 0.1$, $g_5 = \pi\sqrt{2L}$, $\delta m_{1H}^2 \simeq -(0.024/L)^2$, $\delta m_{1\Phi}^2 \simeq -(0.032/L)^2$ and $z_1 = 1 \text{ TeV}^{-1}$. We find that f_1^h is very well approximated by the 0-mode f_0^h obtained with vanishing quartic coupling and suitable boundary masses. Besides in Ap. A we provide approximations for a simple calculation of m_1 and m_2 . A detailed calculation of Higgs couplings and the associated observables must be done for a more quantitative statement about this point of parameter space.

The Higgs interacts with the KK vectors arising from the 5D EW and FN symmetries. For the analysis of flavor violation one needs the coupling with $V^{(0)}$ and $V^{(1)}$:

$$g_{(0n)}^{hh} = \frac{1}{g_5^2} \int dz a(z)^3 f_0^V(z) f_n^V(z) (f_0^h(z))^2 \simeq \frac{g_5}{\sqrt{L}} I_{(0n)}^{hh}(\beta_H) \quad (16)$$

where $f_0^V(z)$ and $f_1^V(z)$ are the KK wave functions of the 0- and 1-modes of a 5D vector, respectively, and $I_{(0n)}^{hh}(\beta_H) \sim \mathcal{O}(1)$ for $\beta_H \gtrsim -0.5$ [49].

4 Spectrum and interactions of leptons

Let us focus now on the fermions, as well as their interactions with the Higgs and the vector resonances. We will show that with a suitable choice of 5D parameters one can naturally obtain the masses of the light neutrinos and charged leptons of Eqs. (10) and (11). We will also identify configurations with small mixing angles in the charged sector, and we will determine the flavor structure of the couplings.

4.1 KK decomposition

We neglect the Yukawa interactions of the 5D fermions and perform a KK decomposition as: $\psi_{L,R}(x^\mu, z) = \sum_n \psi_{L,R}^{(n)}(x^\mu) f_n^{\psi_{L,R}}(z)$. The sum includes a 0-mode only for (++) BCs, leading

to a chiral spectrum of 0-modes that reproduce the lepton sector of the SM, plus three Right handed neutrinos: $N_R^{(0)}$. A generation index for each 5D and 4D fermion field is understood.

For the neutral leptons we will consider only the 0-modes, whereas for the charged leptons we will consider the 0-mode and the first resonance of each 5D fermion, grouping them in the following chiral vectors:

$$\zeta_L^j = (L_L^{E(0),j}, L_L^{E(1),j}, E_L^{(1),j}) , \quad \zeta_R^j = (E_R^{(0),j}, L_R^{E(1),j}, E_R^{(1),j}) . \quad (17)$$

Notice that, taking into account generation indices, the vectors $\zeta_{L,R}$ have nine components, we will use a Latin superscript for generations and a Greek subscript for the KK components explicitly shown in Eq. (17): $\zeta_{L,R\alpha}^j$.

The 4D Yukawa couplings are obtained after integration over the extra dimension of Eq. (3) with the appropriate KK states and the vev of Φ . For the neutral leptons we are interested in the Yukawa coupling involving the 0-modes only:

$$y_N^{jk} = \frac{x_N^{jk}}{g_5^2} \int dz a(z)^5 f_0^{\text{L}_L,j}(z) f_0^{N_R,k}(z) f_0^h(z) \left(\frac{v_{\Phi 4} f_0^\phi(z)}{\Lambda_5} \right)^{\alpha_N^{jk}} , \quad (18)$$

whereas for the charged leptons we consider also the first KK state:

$$y_E^{jk} = \begin{pmatrix} y_{11}^{jk} & 0 & y_{13}^{jk} \\ y_{21}^{jk} & 0 & y_{23}^{jk} \\ 0 & y_{32}^{jk} & 0 \end{pmatrix} , \quad (19)$$

with

$$y_{\alpha\beta}^{jk} = \frac{x_E^{jk}}{g_5^2} \int dz a(z)^5 f_\alpha^{\zeta_L,j}(z) f_\beta^{\zeta_R,k}(z) f_0^h(z) \left(\frac{v_{\Phi 4} f_0^\phi(z)}{\Lambda_5} \right)^{\alpha_E^{jk}} , \quad (20)$$

where the KK wave-functions $f_\alpha^{\psi,j}$ are those corresponding to the modes of Eq. (17). Notice that, to shorten notation, we omit a subindex E in the components of the charged Yukawa matrix.

The couplings of the charged leptons with the first KK neutral vectors, as $Z^{(1)}$ and $F^{(1)}$, are given by:

$$g_L^{jk} = \delta^{jk} \begin{pmatrix} g_{L,11}^j & g_{L,12}^j & 0 \\ g_{L,12}^j & g_{L,22}^j & 0 \\ 0 & 0 & g_{L,33}^j \end{pmatrix} , \quad g_R^{jk} = \delta^{jk} \begin{pmatrix} g_{R,11}^j & 0 & g_{R,13}^j \\ 0 & g_{R,22}^j & 0 \\ g_{R,13}^j & 0 & g_{R,33}^j \end{pmatrix} , \quad (21)$$

where we have factorized from the coupling the non-universal charge: $Q^Z = (T^3 - s_W^2 Q)$ and p , respectively for $Z^{(1)}$ and $F^{(1)}$, and with the following definition:

$$g_{L,\alpha\beta}^j = \frac{1}{g_5^2} \int dz a(z)^4 f_\alpha^{\zeta_L,j}(z) f_\beta^{\zeta_L,j}(z) f_1^V(z) , \quad g_{R,\alpha\beta}^j = g_{L,\alpha\beta}^j (L \rightarrow R) . \quad (22)$$

The flavor structure of the couplings of Eq. (19) can be simplified by considering the following approximations:

$$\begin{aligned}
y_{11}^{jk} &= x_E^{jk} \frac{g_5}{\sqrt{L}} F(1 - 2c_L^j) \delta^{\alpha_E^{jk}} F(1 + 2c_E^k) I_{11}^{jk} , & I_{11}^{jk} &= \frac{F(2 + 2\beta_H) F(2 + 2\beta_\Phi)^{\alpha_E^{jk}}}{F(2 - c_L^j + c_E^k + \beta_H + \alpha_E^{jk}(2 + \beta_\Phi))} , \\
y_{13}^{jk} &\simeq x_E^{jk} \frac{g_5}{\sqrt{L}} F(1 - 2c_L^j) \delta^{\alpha_E^{jk}} I_{13} , & I_{13} &\approx 0.77 , \\
y_{21}^{jk} &\simeq x_E^{jk} \frac{g_5}{\sqrt{L}} \delta^{\alpha_E^{jk}} F(1 + 2c_E^k) I_{21} , & I_{21} &\approx 0.77 , \\
y_{23}^{jk} &\simeq x_E^{jk} \frac{g_5}{\sqrt{L}} \delta^{\alpha_E^{jk}} I_{23} , & I_{23} &\approx 1 , \\
y_{32}^{jk\dagger} &\simeq x_E^{jk} \frac{g_5}{\sqrt{L}} \delta^{\alpha_E^{jk}} I_{32}^\dagger(\alpha_E^{jk}) , & I_{32} &\approx \frac{0.6}{1 + \alpha_E^{jk}} ,
\end{aligned} \tag{23}$$

with:

$$\delta = \frac{g_5}{\sqrt{L}} \frac{v_{\Phi 4} z_1}{L \Lambda_5} . \tag{24}$$

We have checked that corrections to these approximations are below 20% for the region of the parameter space of interest, which will be specified in the next subsection. A few comments are in order. Notice that the 4D Yukawa coupling of Eq. (18) gives the same result as y_{11} in Eq. (23), replacing $E \rightarrow N$. Since the scalars and the KK fermions are localized towards the IR boundary, the integrals with one 0-mode are suppressed when f_0^ψ is localized towards the UV boundary, whereas integrals with two KK fermions (++) are $\mathcal{O}(1)$ and integrals with two KK modes (--) are suppressed for large α , since in this case the support of $(f_0^\phi)^\alpha$ shifts towards the IR boundary where $f_1^{\psi(--)}$ vanishes. Note that for a bulk Higgs, the so-called "wrong" Yukawa coupling y_{32}^{jk} does not vanish; instead, it is misaligned from y_{23}^{jk} while sharing the same hierarchical structure.

Let us focus on y_{11}^{jk} . The factors $F(2 + 2\beta_{H,\Phi})$, as well as the denominator of I_{11}^{jk} , are of $\mathcal{O}(1)$ for the region of parameter space of interest. The factors $F(1 \mp 2c_{L,\psi})$ give an exponential suppression if $\pm c_{L,\psi} > 1/2$, as is well known in theories of flavor in a slice of AdS_5 . The new ingredient is the factor $\delta^{\alpha_E^{jk}}$, that plays the same role as in FN in 4D. By using the estimate for Λ_5 (see sec. 2) and $g_5^2/L = (4\pi)^2/N_{\text{CFT}}$, we obtain:

$$\delta \sim v_{\Phi 4} z_1 \frac{8}{3N_{\text{CFT}}^{3/2}} . \tag{25}$$

We will consider

$$\delta \approx \sqrt{\lambda_C} \approx 0.47 , \tag{26}$$

which, for a natural vev: $v_{\Phi 4} z_1 \sim 1$, requires a small value $N_{\text{CFT}} \simeq 3$, leading to a sizable 5D coupling in the scalar sector.

To simplify the flavor structure of the couplings with $V^{(1)}$, (21), it is useful to consider the

following approximations:

$$\begin{aligned}
g_{L,11}^j &\approx \mathcal{C}_{1,2} \frac{g_5}{\sqrt{L}} \frac{5 - 2c_L^j}{4(2 - c_L^j)(3 - c_L^j)} F(1 - 2c_L^j)^2 , \quad g_{R,11}^j = g_{L,11}^j (c_L \rightarrow -c_E) , \\
g_{L,12}^j &\approx \frac{g_5}{\sqrt{L}} F(1 - 2c_L^j) , \quad g_{R,13}^j = g_{L,12}^j (c_L^j \rightarrow -c_E^j) , \\
g_{L,22}^j &\approx \frac{g_5}{\sqrt{L}} , \quad g_{R,22}^j \approx \frac{g_5}{\sqrt{L}} 0.77 , \\
g_{L,33}^j &\approx \frac{g_5}{\sqrt{L}} 0.77 , \quad g_{R,33}^j \approx \frac{g_5}{\sqrt{L}} , \tag{27}
\end{aligned}$$

where, for $g_{L,R,11}$, we omitted a universal term present in vector fields with (+) BC in the UV, and $\mathcal{C}_{n,2}$ denotes the coefficient of the quadratic term in the expansion around the UV boundary of $f_n^V(z)$: $f_n^V(z) = \mathcal{C}_{n,0} + \mathcal{C}_{n,2}(z - z_0)^2 + \dots$, for which, in the case of the first KK vector, $\mathcal{C}_{1,2} \approx 3.4$. Corrections to these approximations are below 10% for the region of the parameter space of interest.

4.2 Light leptons

To leading order the masses and mixing angles of the light leptons are obtained from the 3×3 mass matrices:

$$m_N^{jk} = v_{H4} y_N^{jk} , \quad m_E^{jk} = v_{H4} y_{11}^{jk} , \tag{28}$$

with the 4D Yukawa couplings defined in Eqs. (18) and (23). See Ap. B for the diagonalization of the mass matrix in KK space.

It is useful to parameterize $m_{N,E}$ in terms of powers of λ_C , to this end we express the degree of compositeness of the 0-modes in powers of λ_C , and we define the corresponding exponent through the following relation:

$$F(1 \mp 2c_{L,\psi}) \equiv \lambda_C^{n_{L,\psi}} . \tag{29}$$

Using Eqs. (26) and (29) in (18) and (23), one gets:

$$m_\psi^{jk} \sim v_{H4} x_\psi^{jk} \frac{g_5}{\sqrt{L}} \lambda^{n_L^j + |p_L^j - p_\psi^j| + n_\psi^k} , \quad \psi = N, E . \tag{30}$$

The eigenvalues and eigenvectors of the the mass matrices of Eq. (30) can be computed perturbatively in powers of λ_C . By choosing suitable values of n_ψ^j and p_{ψ^j} the components of the Yukawa matrix have integer powers of λ_C and it is straightforward to perform these expansions. Very useful approximations can be obtained by considering the following estimates [48]:

$$m_{\psi j} \sim v_{H4} \frac{g_5}{\sqrt{L}} \lambda^{n_L^j + |p_L^j - p_\psi^j| + n_\psi^j} , \tag{31}$$

$$\theta_{\psi_L}^{jk} \sim \lambda^{n_L^j - n_L^k + |p_L^j - p_\psi^k| - |p_L^k - p_\psi^k|} , \quad j < k , \tag{32}$$

$$\theta_{\psi_R}^{jk} \sim \lambda^{n_\psi^j - n_\psi^k + |p_\psi^k - p_\psi^j| - |p_L^k - p_\psi^k|} , \quad j < k , \tag{33}$$

where $m_{\psi j}$ is an eigenvalue and θ_{jk} is a rotation angle. Strictly speaking these approximations are only valid for 2×2 matrices when $m_{11} \ll m_{12}, m_{21}$, however we have checked, by explicitly performing the calculations in powers of λ_C , that in all the cases that we will consider with 3×3 matrices they give the correct result to leading order.

In table 2 we show a set of FN charges and 5D fermion masses that reproduce the neutrino mass matrix of Eq. (10), with:

$$m_{\nu 3} \simeq v_{H4} \frac{g_5}{\sqrt{L}} \lambda_C^{20} . \quad (34)$$

Even though there are many other sets of charges and masses leading to Eq. (10), we have not found any solution with integer charges only, instead at least one of the charges is half-integer. Besides we are interested in configurations with $|c_i| > |c_j|$ for $i < j$, meaning that the lighter generations are more localized towards the UV boundary, and thus have less degree of compositeness, than the heavier ones. Additionally, we are interested in low values of the FN charges, since as we will show in sec. 5, there are flavor transitions that depend on p^2 .

generation	p_L	p_N	c_L	c_N	n_L	n_N
1st	2	1	0.66	-1.25	4	17
2nd	-1	1	0.61	-1.21	3	16
3rd	-3	1/2	0.48	-1.18	1	31/2

Table 2: Benchmark point with FN charges and 5D fermion masses that reproduce the neutrino mass matrix of Eq. (10).

The 5D masses c_N of table 2 strongly localize ν_R of all the generations towards the UV boundary, with values that are similar but not identical. The factor giving the largest suppression of neutrino masses is $F(1 + 2c_\nu)$. The 5D masses c_L generate a moderate suppression for the first and second generations, whereas the Left-handed third generation is only suppressed by $\sim \sqrt{\log(z_1/z_0)}$.

By making use of Eqs. (32) and (33) one can estimate the mixing angles of the neutrino sector, obtaining the values of Eq. (9) for the Left-handed fermions, whereas the Right-handed angles are:

$$\theta_{12}^{\nu_R} \sim \lambda_C , \quad \theta_{23}^{\nu_R} \sim \lambda_C , \quad \theta_{13}^{\nu_R} \sim \lambda_C^2 . \quad (35)$$

Table 3 shows a set of benchmark (BM) points for the charged leptons, defined by FN charges and 5D masses. Together with the parameters of the doublets in Table 2, these points reproduce the charged-lepton masses and lead to suppressed mixing angles $\theta_{E_{L,R}}^{jk}$. The BMs have different values of p_{E3} and n_{E3} , with BM1 having $p_{E3} = -n_{E3} = -3$, and similarly for the subsequent BMs. As we will show in the following sections, some BM points exhibit a parametric suppression of the most constraining flavor observables compared with APC.

generation	p_E	c_E	n_E
1st	1	-0.66	4
2nd	-1	-0.61	3
3rd	$-3, -5/2, -2, -3/2$	$-0.61, -0.58, -0.56, -0.53$	$3, 5/2, 2, 3/2$

Table 3: Benchmark points with FN charges and 5D fermion masses that determine the sector of charged leptons. For the 3rd generation we show four solutions that define four BM points: BM1, BM2, BM3 and BM4.

For the BMs we obtain:

$$m_E \sim \frac{g_5}{\sqrt{L}} v_{H4} \begin{pmatrix} \lambda_C^9 & \lambda_C^{10} & \lambda_C^{12-9} \\ \lambda_C^9 & \lambda_C^6 & \lambda_C^{8-5} \\ \lambda_C^9 & \lambda_C^6 & \lambda_C^4 \end{pmatrix}, \quad (36)$$

where 12–9 (8–5) denotes the values 12, 11, 10, 9 (8, 7, 6, 5) corresponding to BM1–BM4. In Ap. B we show the diagonalization of these matrices perturbatively in powers of λ_C .

It is interesting to compare the size of the rotation angles in the charged sector with APC. Considering the Left-Right symmetric limit: $c_L^j \simeq c_E^j$ [56], the mixing angles in APC are given by $\theta^{jk} \sim \sqrt{m_e^j/m_e^k}$ for $j < k$. By using these estimates as well as Eqs. (32) and (33) for the BM points, we obtain the results of table 4, expressed in terms of $\log_{\lambda_C} \theta^{jk}$. For all the BM points the mixing angles are suppressed in our model compared with APC, with the only exception of $\theta_{e_L}^{23}$ that, for BM4, is of the same order as in APC. $\theta_{e_L}^{12}$, as well as all $\theta_{e_R}^{jk}$, do not change as we change the BM point, whereas $\theta_{e_L}^{23}$ and $\theta_{e_L}^{13}$ depend on the BM, increasing their size from BM1 to BM4.

$\log_{\lambda_C} \theta^{jk}$	$\theta_{e_L}^{12}$	$\theta_{e_L}^{23}$	$\theta_{e_L}^{13}$	$\theta_{e_R}^{12}$	$\theta_{e_R}^{23}$	$\theta_{e_R}^{13}$
APC	1.7	1	2.7	1.7	1	2.7
Model	4	4 – 1	8 – 5	3	2	5

Table 4: Mixing angles in the charged sector expressed as $\log_{\lambda_C} \theta^{jk}$ in APC and in the model. The interval 4 – 1 (8 – 5) means that for BM1, BM2, BM3, BM4 we obtain: 4, 3, 2, 1 (8, 7, 6, 5).

The flavor dependent values of c leads to different KK fermion masses. For the BM points of tables 2 and 3, the mass of the first KK fermion doublet $L^{(1)}$ and singlet $E^{(1)}$ is $m_1 = (2.46 - 2.65)/z_1$, depending on c , with the lightest value for $|c| = 0.48$ and the largest one for $|c| = 0.66$, whereas for $N^{(1)}$ we get $m_1 = (3.39 - 3.49)/z_1$.

4.3 Interactions with resonances in the mass basis

In the next section, we will study the contributions to flavor observables from KK states. Since they receive corrections from the KK mixing, one has to consider the diagonalization of the charged lepton mass matrix. For simplicity we will consider the case of one generation only, the results can be extended to three generations straightforwardly. The mass matrix of the charged leptons of Eq. (17) is given by:

$$M_E = v_{H4} y_E + \text{diagonal}(0, m_1^L, m_1^E) , \quad (37)$$

where y_E is defined in Eq. (19) and the second term is a diagonal 3×3 matrix containing the masses of the first level of charged KK states fermions. M_E can be diagonalized in two steps [49]⁶. (i) Taking the limit of vanishing F , in which case there is no mixing with the 0-modes and only the lower-right 2×2 block of M_E is non-trivial. This block can be diagonalized exactly with a bi-unitary transformation. (ii) Restoring the F dependence to M_E and performing a perturbative diagonalization of the new mass matrix expanding in powers of F , as well as in powers of $g_5 v_{H4} / \sqrt{L} m_{\text{KK}}$. We present a summary of results of the mass matrix diagonalization in Ap. B.

Once the rotation matrices are computed, it is straightforward to obtain the couplings with the Higgs field and with the vector resonances. We will use a tilde to denote masses and couplings of fermions in this basis: \tilde{m}_β , $\tilde{y}_{\alpha\beta}$ and $\tilde{g}_{\alpha\beta}$. The results can be found in Ap. B.

5 Lepton flavor violation

Now we study CP and LFV in our model [57, 58]. Following Ref. [59], we consider dimension six vector and dipole operators, respectively generated at tree and one-loop level. Dimension six scalar and contact operators give subdominant contributions in our model.

Since we are considering massive neutrinos, we will include the effect of neutrino Yukawa couplings in dipole operators, that give contributions by the virtual-exchange of a charged Higgs. The neutrino Yukawa coupling involving one KK neutrino have a flavor structure determined by α_N^{jk} , different from the charged lepton one that depends on α_E^{jk} .

First we present the dimension six operators and match their Wilson coefficients to our model. Then we compare the prediction with the case of APC, in this case we will show the results up to factors of $\mathcal{O}(1)$. We assume maximal CP violating phases.

⁶Notice that in Ref. [49] the basis is ordered differently and the mass matrix is taken symmetric.

5.1 Low energy effective theory for lepton flavor violation

We extend the SM with dimension six operators made of SM fields:

$$\mathcal{L}_{\text{eff}} = \sum_j \hat{C}_j \mathcal{Q}_j . \quad (38)$$

The Wilson coefficients have flavor indices, \hat{C}_j^{kl} , that for the charged leptons take the values e, μ, τ . A complete set of operators can be found, for example, in Ref. [59]. We follow the presentation of that reference.

For this work we are interested in dipole operators

$$\begin{aligned} \mathcal{Q}_{eW} &= \bar{\ell} \sigma^{\mu\nu} e \tau^a W_{\mu\nu}^a H , \\ \mathcal{Q}_{eB} &= \bar{\ell} \sigma^{\mu\nu} e B_{\mu\nu} H , \end{aligned} \quad (39)$$

from which one can obtain the electromagnetic dipole operator

$$\mathcal{Q}_{e\gamma} = \cos \theta_W \mathcal{Q}_{eB} - \sin \theta_W \mathcal{Q}_{eW} . \quad (40)$$

We also consider operators quadratic in the Higgs as well as in the lepton fields, also denoted as vector operators:

$$\begin{aligned} \mathcal{Q}_{H\ell}^{(1)} &= (H^\dagger i \overleftrightarrow{D}_\mu H)(\bar{\ell} \gamma^\mu \ell) , \\ \mathcal{Q}_{H\ell}^{(3)} &= (H^\dagger i \overleftrightarrow{D}_\mu^a H)(\bar{\ell} \gamma^\mu \tau^a \ell) , \\ \mathcal{Q}_{He} &= (H^\dagger i \overleftrightarrow{D}_\mu H)(\bar{e} \gamma^\mu e) , \end{aligned} \quad (41)$$

that after EWSB modify the Z couplings.

Matching the Wilson coefficient of the electromagnetic dipole operator we obtain:

$$\begin{aligned} \hat{C}_{e\gamma}^h &\approx -\frac{e}{(4\pi)^2 v} \sum_{\beta=2,3} \tilde{y}_{1\beta} \frac{1}{\tilde{m}_\beta} \tilde{y}_{\beta 1} , \\ \hat{C}_{e\gamma}^{Z(1)} &\approx -\frac{e}{(4\pi)^2 v} \sum_{\beta=2,3} \tilde{g}_{L,1\beta} \tilde{m}_\beta \tilde{g}_{R,\beta 1} J(\tilde{m}_\beta^2, m_{Z(1)}^2) , \end{aligned} \quad (42)$$

where

$$J(x, y) = \frac{y \log(y/x) + x - y}{(x - y)} \rightarrow \frac{1}{2x} , \quad (43)$$

with the r.h.s corresponding to the limit $y \rightarrow x$. In our estimates and numerical results of secs. 5.2 and 6.2 we will include the contribution to dipole operators arising from the charged Higgs, that depends on y_N and is misaligned with the neutral one, as well as the contribution from $F^{(1)}$, that depends on the FN charges of the fermions.

Matching the Wilson coefficient of vector operators and denoting as Q_β^Z the Z -charge of the fermion β , we get:

$$\begin{aligned}\hat{C}_{H\ell}^{(1)} &\approx \sum_{\beta=2,3} \tilde{y}_{1\beta} \frac{1}{\tilde{m}_\beta} Q_\beta^Z \frac{1}{\tilde{m}_\beta} \tilde{y}_{1\beta}^\dagger + \frac{g_{(0n)}^{hh} \tilde{g}_{L,11}}{m_{Z^{(1)}}^2} , \\ \hat{C}_{H\ell}^{(3)} &= 0 , \\ \hat{C}_{He} &\approx \sum_{\beta=2,3} \tilde{y}_{\beta 1}^\dagger \frac{1}{\tilde{m}_\beta} Q_\beta^Z \frac{1}{\tilde{m}_\beta} \tilde{y}_{\beta 1} + \frac{g_{(0n)}^{hh} \tilde{g}_{R,11}}{m_{Z^{(1)}}^2} .\end{aligned}\quad (44)$$

To analyse the flavor structure of the Wilson coefficients one can expand them to leading order in $F(c)$, $g_5 v_{H4}/\sqrt{L} m_{\text{KK}}$ and $g_{\text{SM}} \sqrt{L}/g_5$, obtaining:

$$\begin{aligned}\hat{C}_{e\gamma}^h &\approx \frac{3e}{(4\pi)^2} y_{13} \frac{1}{m_3} y_{32} \frac{1}{m_2} y_{21} , \\ \hat{C}_{e\gamma}^{Z^{(1)}} &\approx \frac{e}{(4\pi)^2} \frac{1}{2m_{Z^{(1)}}^2} (y_{13} g_{L33} g_{R,13} - g_{L,12} g_{R,22} y_{21} + g_{L,12} y_{23} g_{R,13}) , \\ \hat{C}_{H\ell}^{(1)} &\approx y_{13} \frac{1}{2m_3^2} y_{13}^\dagger + \frac{g_{(0n)}^{hh} \tilde{g}_{L,11}}{m_{Z^{(1)}}^2} , \\ \hat{C}_{He} &\approx -y_{21}^\dagger \frac{1}{2m_2^2} y_{21} + \frac{g_{(0n)}^{hh} \tilde{g}_{R,11}}{m_{Z^{(1)}}^2} .\end{aligned}\quad (45)$$

The flavor structure of the couplings is given in Eqs. (23) and (27).

Finally, one has to rotate to the mass basis in the generation space B:

$$C_{e\gamma} = U_{e_L} \hat{C}_{e\gamma} U_{e_R}^\dagger, \quad C_{H\ell} = U_{e_L} \hat{C}_{H\ell} U_{e_L}^\dagger, \quad C_{He} = U_{e_R} \hat{C}_{He} U_{e_R}^\dagger . \quad (46)$$

5.2 Estimates of the Wilson coefficients and comparison with APC

In this subsection, we compare the Wilson coefficients predicted by our model with those of APC in Ref. [59]. As in sec. 4.2, we consider the Left–Right symmetric limit for APC, in which case the degree of compositeness of the chiral charged leptons is directly determined by their masses [56]. Using Eq. (11), the corresponding Wilson coefficients can then be expanded in powers of λ_C . Also in our model, with $U_{e_{L,R}}$, $F(1 \mp c)$ and δ parameterized in powers of λ_C , the Wilson coefficients admit an expansion in the same parameter.

We obtain the following result for the electron EDM:

$$C_{e\gamma}^e \sim (C_{e\gamma}^e)|_{\text{APC}} \lambda_C^2 , \quad (47)$$

dominated by both, the neutral and the charged Higgs contributions, for the four BM points of table 3. Earlier bounds on the electron EDM implied that in APC $m_{KK}/(g_5/\sqrt{L}) \gtrsim 30 \text{ TeV}$ [60,

61], but the latest results [62, 63] significantly strengthen this constraint to 100–175 TeV. Although the suppression in Eq. (47) lowers the bound on the NP scale by a factor λ_C , obtaining $m_{KK}/(g_5/\sqrt{L}) \gtrsim 22 - 39$ TeV, reaching the TeV scale requires $C_{e\gamma}^e \sim (C_{e\gamma}^e)|_{APC} \lambda_C^6$.

For the flavor violating dipole operators we get:

$$C_{e\gamma}^{\mu e} \sim (C_{e\gamma}^{\mu e})|_{APC} \lambda_C^{3/2}, \quad C_{e\gamma}^{\tau\mu} \sim (C_{e\gamma}^{\tau\mu})|_{APC} \lambda_C^{1,1,1,0}, \quad C_{e\gamma}^{\tau e} \sim (C_{e\gamma}^{\tau e})|_{APC} \lambda_C^{5/2}. \quad (48)$$

In $C_{e\gamma}^{\mu e}$ the dominant contribution is generated by $F^{(1)}$ exchange in the operator with the chiral structure $\bar{\mu}_L \sigma^{\nu\rho} e_R$, whereas the operator with flipped chiralities is suppressed by an extra factor λ_C . Experimental bounds require in APC $m_{KK}/(g_5/\sqrt{L}) \gtrsim 32$ TeV [64], the suppression in the first line of Eq. (48) lowers the bound to ~ 10 TeV. In $C_{e\gamma}^{\tau\mu}$ the dominant contribution for the first three BM points is dominated by neutral Higgs and $F^{(1)}$ virtual exchange in the operator with the chiral structure $\bar{\tau}_L \sigma^{\nu\rho} \mu_R$ and is suppressed by λ_C compared with APC. For BM4 the dominant operator is $\bar{\mu}_L \sigma^{\nu\rho} \tau_R$, all the contributions are of the same order and there is no suppression. Finally, $C_{e\gamma}^{\tau e}$ is dominated by $F^{(1)}$ exchange in the operator with the chiral structure $\bar{\tau}_L \sigma^{\nu\rho} e_R$ for all the BM points, with a suppression factor $\lambda_C^{5/2}$ compared with APC. For BM4 there are contributions of the same order from $F^{(1)}$ in the chiral flipped operator and from Higgs exchange.

For the vector operators in μe transitions we obtain the following results:

$$C_{H\ell}^{(1)\mu e} \sim (C_{H\ell}^{(1)\mu e})|_{APC} \lambda_C^{5/2}, \quad C_{He}^{\mu e} \sim (C_{He}^{\mu e})|_{APC} \lambda_C^{3/2}. \quad (49)$$

For $C_{H\ell}^{(1)\mu e}$ both terms of Eq. (45) result of the same order in powers of λ_C , whereas for $C_{He}^{\mu e}$ the second one dominates. The suppression compared with APC relaxes the bound on $m_{KK}/(g_5/\sqrt{L})^{1/2}$, from 3 TeV [59, 64] to 0.5 TeV.

For $\tau\mu$ vector operators we get:

$$C_{H\ell}^{(1)\tau\mu} \sim (C_{H\ell}^{(1)\tau\mu})|_{APC} \lambda_C^{1,1,-1,-1}, \quad C_{He}^{\tau\mu} \sim (C_{He}^{\tau\mu})|_{APC} \lambda_C^{3,2,1,0}, \quad (50)$$

where the list of exponents refers to the list of BM points, from 1 to 4. For $C_{H\ell}^{(1)\tau\mu}$ the second term of Eq. (45) dominates, whereas for $C_{He}^{\tau\mu}$ both are of the same order. The present bounds on decays mediated by these operators do not give relevant constraints in the model.

Finally, for τe vector operators we get:

$$C_{H\ell}^{(1)\tau e} \sim (C_{H\ell}^{(1)\tau e})|_{APC} \lambda_C^{7/2,7/2,5/2,5/2}, \quad C_{He}^{\tau e} \sim (C_{He}^{\tau e})|_{APC} \lambda_C^{9/2,7/2,5/2,3/2}, \quad (51)$$

where again the list of exponents correspond to the BM points, from 1 to 4. In all the cases the second term of Eq. (45) dominates, except for BM1 and 2 in $C_{H\ell}^{(1)\mu e}$, where the first term is of the same order in powers of λ_C .

6 Numerical results

In this section, we present the numerical results obtained within the model for BM1. The 5D parameters are specified as follows. The 5D fermion masses are given in table 2, together with

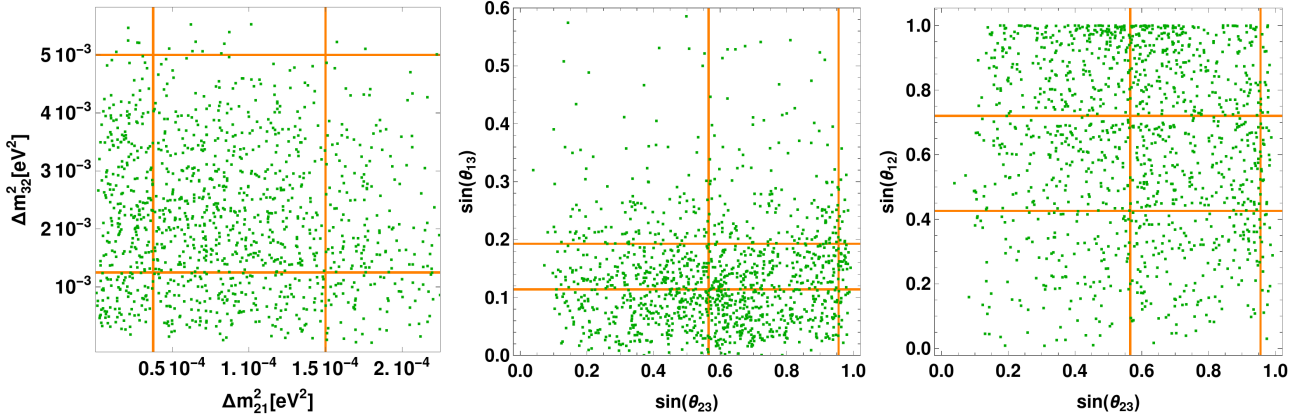


Figure 2: Numerical predictions of the neutrino observables with BM1 of the model, performing a random scan over the Yukawa couplings. On the left we show the mass-squared differences and in the centre and in the right the mixing angles of the PMNS matrix.

the BM1 point of the charged-lepton sector defined in table 3. The 5D coupling in the fermion sector is fixed to $g_5/\sqrt{L} = 3$. For the scalar fields we set $\beta_\Phi = \beta_H = 0$. In addition, we choose $\delta = \sqrt{\Lambda_C}$, $z_0 = 10^{-15}z_1$, and $z_1 = 1/\text{TeV}$. A random scan is then performed over the $\mathcal{O}(1)$ parameters of the model, namely the coefficients x_N^{jk} and x_E^{jk} of the 5D Yukawa couplings in Eq. (3), restricted to the range $|x_{N,E}^{jk}| \in (1/3, 3)$.

We do not aim to fit the lepton observables with precision, instead we will show that the chosen scenario can naturally reproduce masses and mixing angles close to the observed values. Given a set of parameters that is closed to the measured values, by small adjustments of the parameters one can reproduce them with precision.

We present first the predictions for the masses and mixing angles of the light leptons, and then we show the results for the Wilson coefficients of the flavor- and CP-violating operators.

6.1 Lepton masses and mixing angles

In Fig. 2 we show the results for the neutrino mass squared differences and the mixing angles of the PMNS matrix. The plot on the left displays Δm_{ij}^2 with the orange lines corresponding to departures by a factor 1.5 from the measured values, whereas the plots on the centre and on the right show $\sin \theta_{ij}$ with the orange line corresponding to a tolerance factor 1.3. From the random scan, the mean value and standard deviation of the mass-squared differences are: $\Delta m_{21}^2 = (9.7 \pm 6.7) \times 10^{-5} \text{ eV}^2$ and $\Delta m_{32}^2 = (2.2 \pm 1.2) \times 10^{-3} \text{ eV}^2$, while the mixing angles are: $|\sin \theta_{12}| \approx 0.64 \pm 0.27$, $|\sin \theta_{23}| \approx 0.58 \pm 0.24$ and $|\sin \theta_{13}| \approx 0.14 \pm 0.09$.

In Fig. 3 we present the results for the charged lepton masses. The green points correspond to randomly generated samples, while the red points show a subset of the scan that satisfies the neutrino-sector constraints, allowing deviations within a factor of 2 for the measured values of Δm_{kj}^2 and within a factor of 1.3 for $\sin \theta_{jk}$. The orange lines indicate $m_i/2$ and $2m_i$, with

$i = e, \mu, \tau$ denoting the electron, muon, and tau masses, respectively. As expected, no structure is observed for the red points, since the neutrino masses and mixings depend on x_N^{jk} , while the charged ones depend on x_E^{jk} . Although the masses turn out somewhat larger than their physical values on average, a more accurate agreement can be achieved by selecting slightly different values of c_E^j , for example by decreasing n_E^j by 1/2, provided we allow for non-integer n_E^j .⁷

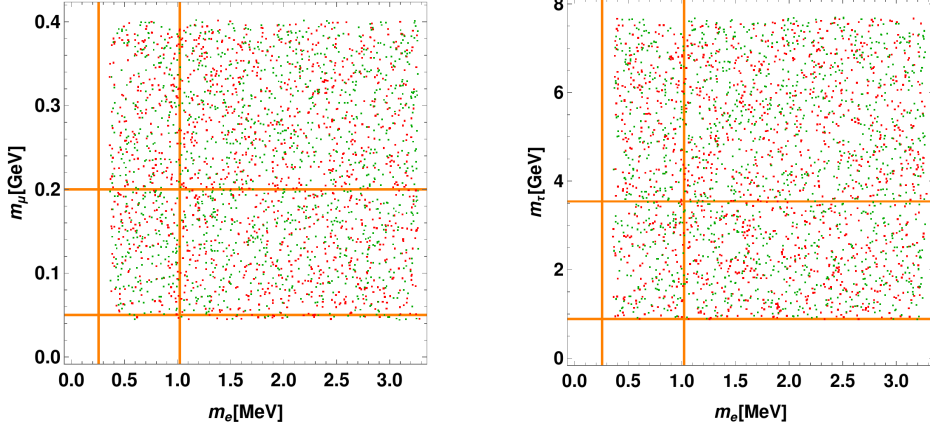


Figure 3: Numerical predictions of the masses of the charged leptons with BM1 of the model, performing a random scan over the Yukawa couplings. Orange lines show the analytical estimates.

6.2 Numerical results for the Wilson coefficients

In this subsection we present the model’s numerical predictions in the case of BM1 for the Wilson coefficients, normalized to the prediction of APC in the Left-Right symmetric limit: $|C/C_{\text{APC}}|$.

Figure 4 presents the prediction for dipole operators. The results from a random parameter scan are shown as green points, with a subset of these points that reproduce the experimental masses and mixing of neutrinos highlighted in red.⁸ The distributions of both sets show no appreciable difference. For reference, the analytical estimates (Eqs. (47-51)) are indicated by orange lines, with the gray lines corresponding to $C = C|_{\text{APC}}$. The cusps visible in the upper-right region of the distributions correspond to the maximum values of the Yukawa couplings allowed in the scan.

The top-left panel displays the contributions to the electron EDM operator, $C_{e\gamma}^e$, with the neutral Higgs contribution on the x -axis and the charged Higgs contribution on the y -axis. Compared to the estimate in Eq. (47), the neutral Higgs contribution is larger for some points,

⁷It is not necessary to restrict n_ψ^j to integer values, this choice was adopted to simplify the calculation of the eigenvalues and eigenvectors of the mass matrix, expanded in series in powers of λ_C .

⁸Selecting from them the points that reproduce the masses of the charged leptons withing corrections by a factor 2 does not give significant changes in the distributions of points.

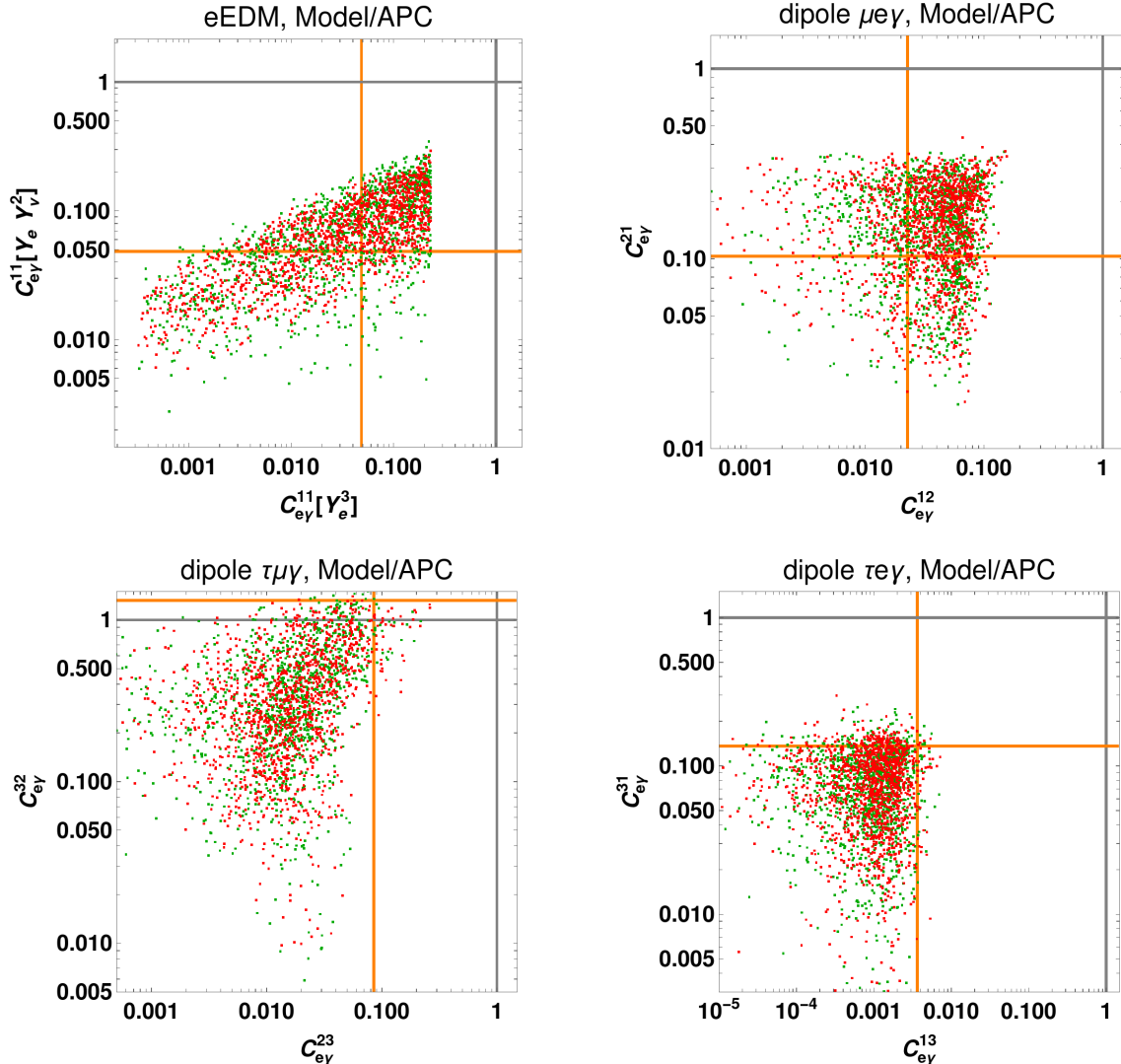


Figure 4: Numerical predictions of the Wilson coefficients of dipole operators with BM1 of the model, normalized with respect to APC, performing a random scan over the Yukawa couplings. Orange lines show the analytical estimates. On the top-left panel we show the neutral and charged Higgs contributions to the e EDM, on the top-right we show the different chiralities in $\mu \rightarrow e\gamma$, as on the bottom-left and bottom-right panels, where we show respectively $\tau \rightarrow \mu\gamma$ and $\tau \rightarrow e\gamma$.

whereas for others the total value of $C_{e\gamma}^e$ is an order of magnitude smaller than the estimate, presumably due to accidental numerical cancellations. The mean value and standard deviation of the points are: 0.066 ± 0.068 and 0.080 ± 0.058 , in the x - and y -axis, respectively, of the same order of magnitude as the estimate $\lambda_C^2 \simeq 0.048$.

The top-right panel shows both chiral structures of $C_{e\gamma}^{\mu e}$. Many points cluster slightly above the estimate, within a factor $\sim 3 - 5$, and a small subset are suppressed by approximately one order of magnitude. The mean value and standard deviation of the coordinates of the points

are: 0.043 ± 0.026 and 0.16 ± 0.08 , of the same size as the respective estimates $\lambda_C^{5/2} \simeq 0.023$ and $\lambda_C^{3/2} \simeq 0.10$.

The bottom-left panel displays $C_{e\gamma}^{\tau\mu}$ for both chiral structures. In this case the orange lines represent analytical estimates that include sizable numerical factors obtained in the full calculation: $C_{e\gamma}^{\tau\mu,23}/(C_{e\gamma}^{\tau\mu,23})_{\text{APC}} \sim (p_{E3}p_{L3} - p_{E2}p_{L2})\lambda_C^3 \approx 0.085$ and $C_{e\gamma}^{\tau\mu,32}/(C_{e\gamma}^{\tau\mu,32})_{\text{APC}} \sim p_{L3}(p_{E3} - p_{E2})\lambda_C \approx 1.32$. These factors derived from the FN charge in the vertices of the one loop diagram explain why the predicted coefficients can reach the APC reference value, even after accounting for the Cabibbo angle suppression. They also show how large charges can increase the LFV dipole. The mean value and standard deviation of the coordinates of the points are somewhat smaller than the estimates: 0.022 ± 0.021 and 0.40 ± 0.30 .

Finally, the bottom-right panel presents $C_{e\gamma}^{\tau e}$. Including the numerical prefactors determined by the FN charges the orange lines are given by: $C_{e\gamma}^{\tau e,13}/(C_{e\gamma}^{\tau e,13})_{\text{APC}} \sim p_{E3}(p_{L3} - p_{L1})\lambda_C^{11/2} \approx 3.6 \times 10^{-3}$ and $C_{e\gamma}^{\tau e,31}/(C_{e\gamma}^{\tau e,31})_{\text{APC}} \sim p_{L3}(p_{E3} - p_{E1})\lambda_C^{5/2}/2 \approx 0.14$. The mean value and standard deviation of the coordinates of the points are a factor 2-3 smaller: $(1.2 \pm 0.9) \times 10^{-3}$ and 0.076 ± 0.043 .

Figure 5 presents the Wilson coefficients for the vector operators, normalized to the APC prediction and using the same color scheme as Fig. 4. The upper-left panel displays the results for μe transitions. The mean value and standard deviation of the coordinates of the points are: 0.025 ± 0.022 and 0.10 ± 0.08 , closely aligned with the analytical estimates of $\lambda_C^{5/2} \approx 0.023$ and $\lambda_C^{3/2} \approx 0.10$, respectively.

The upper-right panel, corresponding to $\tau\mu$ transitions, yields mean values of 0.33 ± 0.62 and 0.009 ± 0.010 . These are consistent with the respective estimates of λ_C and $\lambda_C^3 \approx 0.011$, noting the large standard deviation for the first coordinate.

Finally, the bottom panel shows the prediction for τe transitions. The the observed values $(1.4 \pm 1.3) \times 10^{-2}$ and $(1.4 \pm 1.4) \times 10^{-3}$ can be compared with the estimates $\lambda_C^{7/2} \approx 0.4 \times 10^{-2}$ and $\lambda_C^{9/2} \approx 1.1 \times 10^{-3}$, observing an enhancement by a factor 3 for the first coordinate.

7 Discussions and conclusions

One of the main goals of particle physics is to find an explanation of the pattern of flavor of the SM. In the present paper we have presented a 5D model capable of explaining the flavor of the leptonic sector. The model incorporates two principal mechanisms: partial compositeness, achieved through the localization of zero modes along the extra dimension, and a bulk horizontal U(1) gauge symmetry, under which the 5D leptons are charged. We added a 5D scalar field Φ and an IR boundary potential that triggers EW and U(1) spontaneous symmetry breaking. Obtaining a U(1) symmetry breaking parameter of order $\sqrt{\lambda_C}$ requires a rather large 5D coupling in the scalar sector of the theory, dual to $N_{\text{CFT}} \simeq 3$. 5D Yukawa interactions are generated by higher dimensional operators with powers of Φ/Λ determined by the fermion

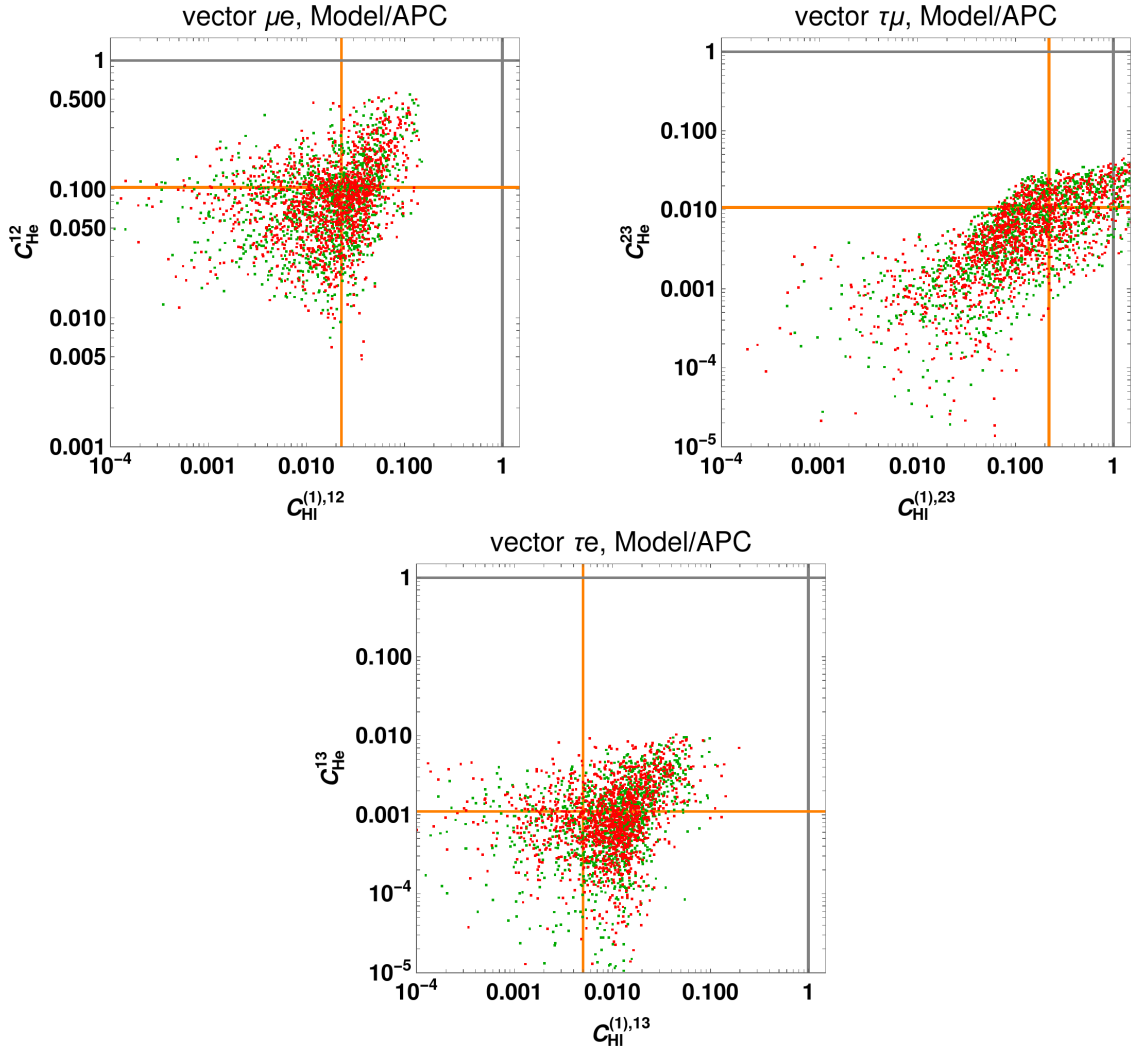


Figure 5: Numerical predictions of the Wilson coefficients of vector operators with BM1 of the model, normalized with respect to APC, performing a random scan over the Yukawa couplings. Orange lines show the analytical estimates. On the top-left and top-right panels we show the results for μe and $\tau \mu$ operators, respectively, and on the bottom one for τe .

charges. In this way, starting from 5D anarchic Yukawa couplings, effective 5D Yukawa interactions with non-trivial flavor patterns are generated, as usual in 4D FN models. We have shown that under the interplay of both mechanisms it is possible to explain the hierarchy of masses of the light leptons, to be identified with the SM ones, as well as the angles of the PMNS matrix. The neutrinos are realized as Dirac fermions, with normal ordered masses and a hierarchical spectrum, and their mixing angles dominate the PMNS matrix. The strong localization of $\nu_R^{(0)}$ towards the UV boundary suppresses the neutrino masses.

We have computed the main contributions to CP and LFV processes, that are dominated by vector and dipole operators generated at tree and one loop level, respectively. There is a new contribution to dipole operators compared with APC, obtained by the exchange of U(1) KK

resonances that, given the non-universal charges of the fermions, is misaligned with the mass. This contribution is the dominant one for LFV dipoles. We have found configurations of charges and masses of the 5D fermions that are capable of suppressing these processes compared with APC. In particular, the e EDM can be suppressed by λ_C^2 , relaxing the bound of APC, but still requiring a compositeness scale $m_*/g_* \gtrsim 22 - 39$ TeV. The bound from $\mu \rightarrow e\gamma$ can be relaxed by a factor $\mathcal{O}(3)$, leaving the compositeness scale in the ballpark of 10 TeV. For $\mu \rightarrow 3e$, induced by vector operators, we get an suppression by a factor $\mathcal{O}(6)$, obtaining $m_* \gtrsim 0.5\sqrt{g_*}$ TeV.

We have also studied the predictions of the model at numerical level. We have performed a random numerical scan over the $\mathcal{O}(1)$ parameters of the theory, namely the coefficients of the 5D Yukawa couplings, finding that the masses and mixing angles of the SM leptons can be naturally obtained. We have also studied the Wilson coefficients of CP and LFV operators, finding good agreement with the estimates.

The model provides a well motivated and computable framework for the study of an extended scalar sector. As we have shown, the radial components of H and Φ mix in 5D, introducing corrections to the Higgs interactions. It would be interesting to study the phenomenology of the light scalars, as well as the axion-like state in the present framework. Moreover, one can study the case of the Higgs as a hologram of A_5 , in which case the Higgs potential is generated at loop level. We leave this subjects for future work.

Our analysis omitted higher-dimensional operators, besides those of \mathcal{L}_y . One could analyse the effect of other higher dimensional operators, as for example corrections to fermionic kinetic terms. That study is beyond the scope of our work.

It is straightforward to extend the framework to include the quark sector. An analysis in a two-site theory has been conducted in Ref. [48]. It would be valuable to study the 5D description, as it offers greater predictive power.

Acknowledgments

This work has been partially supported by CONICET, project PIP-11220200101426, and CNEA scholarships. We thank Esteban Roulet for discussions in the initial stages of the project.

A KK decomposition of the scalar fields

In this appendix we describe the KK decomposition of the scalar fields.

A.1 Vacuum expectation values

The IR potential V_1 triggers spontaneous breaking of both the EW and FN symmetries, while preserving $U(1)_{\text{em}}$, inducing the vevs $v_H(z)$ and $v_\Phi(z)$. Solving the bulk equations of motion for these vev profiles one gets:

$$v_\chi = b_\chi z^{2-\beta_\chi} + c_\chi z^{2+\beta_\chi}, \quad \beta_\chi = \sqrt{4 + m_\chi^2 L^2}, \quad \chi = H, \Phi, \quad (52)$$

where b_χ and c_χ are integration constants that depend on the BCs.

The UV and IR BCs are given by:

$$\left. \left(\partial_z v_\chi + g_5^2 a \frac{\partial}{\partial v_\chi} V_i \right) \right|_{z_i} = 0, \quad \chi = H, \Phi, \quad i = 0, 1. \quad (53)$$

where the UV BCs are evaluated at $z_i = z_0$ and the IR ones at $z_i = z_1$.

The UV BCs depend on the UV masses, we choose them to select the second solution of Eq. (52):

$$2 + \beta_\chi + 2g_5^2 L m_{0\chi}^2 = 0, \quad \chi = H, \Phi, \quad (54)$$

leading to $b_\chi = 0$.

The IR BCs are given by:

$$\left[\partial_z v_H + g_5^2 a (m_{1H}^2 v_H + 4\lambda_{1H} v_H^3 + 2\lambda_{1\Phi H} v_H^2 v_\Phi) \right]_{z_1} = 0, \quad (55)$$

$$\left[\partial_z v_\Phi + g_5^2 a (m_{1\Phi}^2 v_\Phi + 4\lambda_{1\Phi} v_\Phi^3 + 2\lambda_{1\Phi H} v_\Phi^2 v_H) \right]_{z_1} = 0. \quad (56)$$

For suitable choices of the IR masses and couplings c_H and c_Φ do not vanish.

We find it useful to define an IR boundary mass:

$$\delta m_{1\chi}^2 \equiv m_{1\chi}^2 + \frac{2 + \beta_\chi}{2g_5^2 L}. \quad (57)$$

For $\delta m_{1\chi}^2 = 0$ and vanishing quartic couplings one obtains the usual conditions for the existence of a scalar 0-mode.

Following Ref. [55] we define 4D vevs as the integrals of the 5D ones along the extra-dimension:

$$v_{\chi 4}^2 = \frac{1}{g_5^2} \int dz a(z)^3 v_\chi(z)^2, \quad \chi = H, \Phi. \quad (58)$$

Thus the 5D vevs are given by:

$$v_\chi(z) = v_{\chi 4} \frac{g_5}{\sqrt{L}} \frac{z_1}{L} \left(\frac{z}{z_1} \right)^{2+\beta_\chi} F(2 + 2\beta_\chi), \quad (59)$$

where the function $F(x)$ is defined by:

$$F(x) = \left[\frac{x}{1 - (z_0/z_1)^x} \right]^{1/2}. \quad (60)$$

The relation between the 4D vevs and the parameters of the IR potential is given by:

$$v_{H4} = \frac{L}{z_1} \left(\frac{-2\lambda_{1\Phi}\delta m_{1H}^2 + \lambda_{1\Phi H}\delta m_{1\Phi}^2}{4\lambda_{1\Phi}\lambda_{1H} - \lambda_{1\Phi H}^2} \right)^{1/2} \frac{1}{F(2+2\beta_H)}, \quad (61)$$

$$v_{\Phi 4} = \frac{L}{z_1} \left(\frac{-2\lambda_{1H}\delta m_{1\Phi}^2 + \lambda_{1\Phi H}\delta m_{1H}^2}{4\lambda_{1\Phi}\lambda_{1H} - \lambda_{1\Phi H}^2} \right)^{1/2} \frac{1}{F(2+2\beta_\phi)}. \quad (62)$$

The 4D vevs are expected to be of order $1/z_1$.

A.2 Light states

There are scalar physical states, that in general are massive and are a mixture of H and Φ . We consider in this section the lightest states, that would be 0-modes for $\delta m_{1\chi}^2 = 0$ and vanishing boundary quartic couplings. Below we present the KK decomposition of the scalar sector, as well as an approximation taking into account only the would be 0-modes, neglecting the mixing with the heavier KK states.

Expressing the 5D scalar fields as $H^t = (0, (v_H + h)/\sqrt{2})$ and $\Phi = (v_\Phi + \phi)/\sqrt{2}$, one obtains, for the physical fields h and ϕ , bulk equations of motion without mixing⁹:

$$[(p^2 + a^{-3}\partial_z a^3 \partial_z - a^2 m_\chi^2)\chi] = 0, \quad \chi = h, \phi. \quad (63)$$

The UV BCs are given by

$$[(\partial_z + 2g_5^2 a m_{0\chi}^2)\chi] \Big|_{z_0} = 0, \quad \chi = h, \phi. \quad (64)$$

On the other hand, the IR BCs mix both fields:

$$\{[\partial_z + a(2m_{1H}^2 + 12\lambda_{1H}v_H^2 + 2\lambda_{1\Phi H}v_\Phi^2)]h + 4a\lambda_{1\Phi H}v_\Phi v_H\phi\} \Big|_{z_1}, \quad (65)$$

$$\{[\partial_z + a(2m_{1\Phi}^2 + 12\lambda_{1\Phi}v_\Phi^2 + 2\lambda_{1\Phi H}v_H^2)]\phi + 4a\lambda_{1\Phi H}v_\Phi v_Hh\} \Big|_{z_1}. \quad (66)$$

We decompose the 5D scalars fields in KK modes as:

$$h = \sum_n s^{(n)}(x^\mu) f_n^h(z), \quad \phi = \sum_n s^{(n)}(x^\mu) f_n^\phi(z), \quad (67)$$

with the normalization condition:

$$\frac{1}{g_5^2} \int dz a(z)^3 [f_n^h(z) f_m^h(z) + f_n^\phi(z) f_m^\phi(z)] = \delta_{nm} \quad (68)$$

and KK wave functions given by:

$$f_n^h(z) = \frac{z^2}{N_n^h} [J_{\beta_H}(m_n z) + b_n^h Y_{\beta_H}(m_n z)], \quad f_n^\phi(z) = \frac{z^2}{N_n^\phi} [J_{\beta_\phi}(m_n z) + b_n^\phi Y_{\beta_\phi}(m_n z)], \quad (69)$$

⁹Tadpoles are also absent [55].

where $b_n^{h,\phi}$ are integration constants, $N_n^{h,\phi}$ are normalization factors and we have used $p^2 = m_n^2$ in Eq. (63). Since V_1 induces masses for the KK modes, in general the sums of Eqs. (67) run over $n > 0$.

One can use, for example, Eqs. (64) to obtain the integration constants. The spectrum of scalar states, m_n , can then be obtained from Eqs. (65) and (66), and can be written as:

$$(\partial_z f_n^h + \tilde{m}_{1h} f_n^h)(\partial_z f_n^\phi + \tilde{m}_{1\phi} f_n^\phi) \Big|_{z_1} = \tilde{m}_{1\phi h} \tilde{m}_{1h\phi} f_n^h f_n^\phi \Big|_{z_1} , \quad (70)$$

where:

$$\tilde{m}_{1h} = a(2m_{1H}^2 + 12\lambda_{1H}v_H^2 + 2\lambda_{1\Phi H}v_\Phi^2) \Big|_{z_1} , \quad (71)$$

$$\tilde{m}_{1\phi} = a(2m_{1\Phi}^2 + 12\lambda_{1\Phi}v_\Phi^2 + 2\lambda_{1\Phi H}v_H^2) \Big|_{z_1} , \quad (72)$$

$$\tilde{m}_{1\phi h} = \tilde{m}_{1h\phi} = 4a\lambda_{1\Phi H}v_\Phi v_H h \Big|_{z_1} . \quad (73)$$

Notice that Eq. (70) does not depend on the normalization factor of the KK wave functions. For $\lambda_{1\Phi H} = 0$ the mixing vanishes and Eq. (70) has two sets of solutions that reproduce the spectrum of two independent scalar fields.

One can compute the spectrum of scalar states by considering a perturbative expansion in insertions of the IR boundary terms, the so called zero mode approximation. We first solve for the 0-modes obtained when $\delta m_{1H}^2 = \delta m_{1\Phi}^2 = 0$ and all the quartics vanish: $\lambda_{1H} = \lambda_{1\Phi} = \lambda_{1\Phi H} = 0$, and then we define a mass matrix of the 0-modes that accounts for the effect of those terms of the IR potential. The 0-modes are given by:

$$f_0^\chi(z) = \frac{g_5}{\sqrt{L}} \frac{z_1}{L} \left(\frac{z}{z_1} \right)^{2+\beta_\chi} F(2+2\beta_\chi) , \quad \chi = h, \phi. \quad (74)$$

In terms of these 0-modes one can define a mass matrix as follows:

$$M_s^2 = 2a^4 \left(\begin{array}{cc} (\delta m_{1H}^2 + 6\lambda_{1H}v_H^2 + \lambda_{1\Phi H}v_\Phi^2)(f_0^h)^2 & 2\lambda_{1\Phi H}v_\Phi v_H f_0^h f_0^\phi \\ 2\lambda_{1\Phi H}v_\Phi v_H f_0^h f_0^\phi & (\delta m_{1\Phi}^2 + 6\lambda_{1\Phi}v_\Phi^2 + \lambda_{1\Phi H}v_H^2)(f_0^\phi)^2 \end{array} \right) \Big|_{z_1} . \quad (75)$$

This approximation does not take into account the mixing with the massive modes induced by the IR potential, however for the region of the parameter space we are interested in the corrections are small, as can be seen in Fig. 6, for a suitable choice of parameters. For m_1 the differences between the full calculation and the approximation are below 3%, whereas for m_2 they are below 20%. As usual, obtaining a suppression in the Higgs mass requires tuning of the quartic coupling.

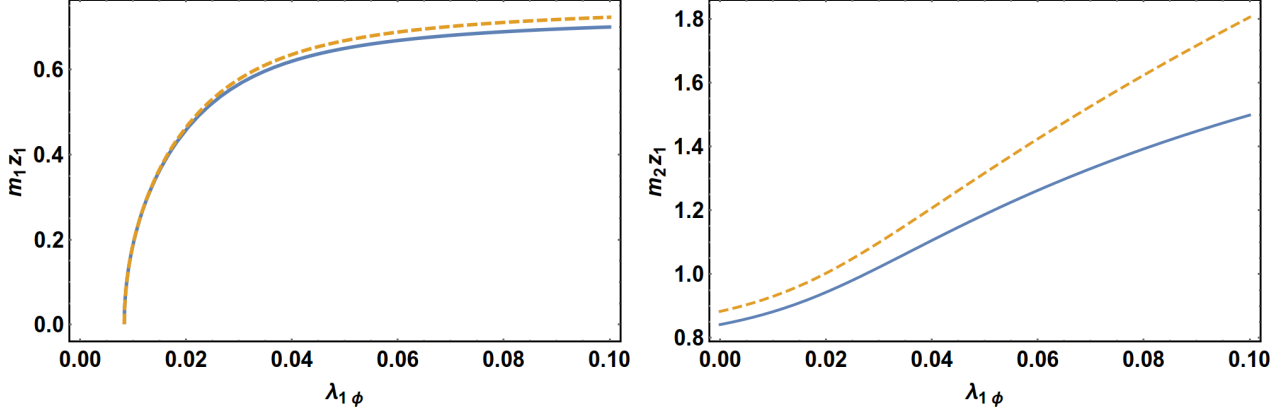


Figure 6: Masses of the first (left panel) and second (right panel) KK scalar modes as function of the quartic coupling $\lambda_{1\Phi}$ for the BM point, in solid blue we show the full expression of Eq. (70) and in dashed orange the formula derived from the approximation of Eq. (75).

B Fermion matrix diagonalization

We consider first the simple case of just one generation. From Eq. (19) the mass matrix of the charged leptons is (37):

$$M_E = \begin{pmatrix} v_{H4}y_{11} & 0 & v_{H4}y_{13} \\ v_{H4}y_{21} & m_1^L & v_{H4}y_{23} \\ 0 & v_{H4}y_{32} & m_1^E \end{pmatrix},$$

$$\sim \begin{pmatrix} \frac{g_5}{\sqrt{L}}v_{H4}F(1-2c_L)F(1+2c_E)\delta^{\alpha_E} & 0 & \frac{g_5}{\sqrt{L}}v_{H4}F(1-2c_L)\delta^{\alpha_E} \\ \frac{g_5}{\sqrt{L}}v_{H4}F(1+2c_E)\delta^{\alpha_E} & m_1^L & \frac{g_5}{\sqrt{L}}v_{H4}\delta^{\alpha_E} \\ 0 & \frac{g_5}{\sqrt{L}}v_{H4}\delta^{\alpha_E} & m_1^E \end{pmatrix}, \quad (76)$$

where m_1^L and m_1^E are the masses of the first KK states, respectively $L^{(1)}$ and $E^{(1)}$. Since $\delta^{\alpha_E} \ll 1$ only if $\alpha_E > 0$, a condition that is not always satisfied once flavor is introduced, we will not expand in powers of δ . Instead we will expand in powers of $F(1-2c_L)$ and $F(1+2c_E)$.

We consider M_E to zeroth order in $F(1 \mp 2c_{L,E})$

$$M_E^{(0)} = \begin{pmatrix} 0 & 0 & 0 \\ 0 & m_1^L & v_{H4}y_{23} \\ 0 & v_{H4}y_{32} & m_1^E \end{pmatrix}, \quad (77)$$

and we perform a diagonalization of $M_E^{(0)}$ with a bi-unitary transformation:

$$M_E^{(1)} = U_L^{(0)\dagger} M_E^{(0)} U_R^{(0)}, \quad (78)$$

where

$$M_E^{(1)} = \text{diag}(0, m_1', m_1''), \quad U_{L,R}^{(0)} = \begin{pmatrix} 1 & 0 & 0 \\ 0 & \cos \theta_{L,R}^{(0)} & -\sin \theta_{L,R}^{(0)} \\ 0 & \sin \theta_{L,R}^{(0)} & \cos \theta_{L,R}^{(0)} \end{pmatrix}. \quad (79)$$

It is straightforward to compute m'_1 , m''_1 and $\sin \theta_{L,R}^{(0)}$.

Armed with these unitary matrices we perform a rotation of M_E as follows:

$$M'_E = U_L^{(0)\dagger} M_E U_R^{(0)} = \begin{pmatrix} v_{H4} y_{11} & \sin \theta_R^{(0)} v_{H4} y_{13} & \cos \theta_R^{(0)} v_{H4} y_{13} \\ \cos \theta_L^{(0)} v_{H4} y_{21} & m'_1 & 0 \\ -\sin \theta_L^{(0)} v_{H4} y_{21} & 0 & m''_1 \end{pmatrix}, \quad (80)$$

and we diagonalize M'_E with a new bi-unitary transformation, calling \tilde{M}_E the diagonal mass matrix:

$$\tilde{M}_E = U_L'^\dagger M'_E U_R'. \quad (81)$$

The matrix of Yukawa couplings is given by:

$$\tilde{y}_E = U_L'^\dagger U_L^{(0)\dagger} y_E U_R^{(0)} U_R'. \quad (82)$$

with y_E given in Eq. (19), restricted to one generation. The matrices of couplings with the first KK vector are:

$$\tilde{g}_L = U_L'^\dagger U_L^{(0)\dagger} g_L U_L^{(0)} U_L', \quad \tilde{g}_R = U_R'^\dagger U_R^{(0)\dagger} g_R U_R^{(0)} U_R'. \quad (83)$$

It is straightforward to obtain the eigenvalues, the rotation matrices and the matrices of couplings performing an expansion in powers of $F(1 \mp 2c_{L,E})$. Simple expressions can be obtained expanding also in powers of v_{H4} . Taking the limit $m_1^L = m_1^R \equiv m_{\text{KK}}$, the eigenvalues are given by:

$$\begin{aligned} \tilde{m}_1 &\approx v_{H4} y_{11} + \frac{v_{H4}^3}{m_{\text{KK}}^2} y_{13} y_{32} y_{21} + \dots, \\ \tilde{m}_{2,3} &\approx m_{\text{KK}} \mp \frac{1}{2} v_{H4} (y_{23} + y_{32}) + \frac{v_{H4}^2}{8m_{\text{KK}}} (y_{23} - y_{32})^2 + \frac{v_{H4}^2}{4m_{\text{KK}}} (y_{13}^2 + y_{21}^2) + \dots \end{aligned} \quad (84)$$

where m_1 is the mass of the would be 0-modes, and $m_{2,3}$ are the masses of the first level of resonances. We have expanded to second order in v_{H4}/m_{KK} and we show also the leading order correction in $F(1 \mp 2c_{L,E})$ for the resonances. The rotation matrices can be expanded as:

$$\begin{aligned} U'_L &\approx \begin{pmatrix} 1 - \frac{v_{H4}^2 y_{13}^2}{2m_{\text{KK}}^2} & \frac{v_{H4} y_{13}}{\sqrt{2}m_{\text{KK}}} + \frac{y_{13}(y_{23}+3y_{32})v_{H4}^2}{4\sqrt{2}m_{\text{KK}}^2} & \frac{v_{H4} y_{13}}{\sqrt{2}m_{\text{KK}}} - \frac{v_{H4}^2 y_{13}(y_{23}+3y_{32})}{4\sqrt{2}m_{\text{KK}}^2} \\ -\frac{v_{H4} y_{13}}{\sqrt{2}m_{\text{KK}}} - \frac{v_{H4}^2 y_{13}(y_{23}+3y_{32})}{4\sqrt{2}m_{\text{KK}}^2} & 1 - \frac{v_{H4}^2 y_{13}^2}{4m_{\text{KK}}^2} & \frac{v_{H4}(y_{13}^2-y_{21}^2)}{4m_{\text{KK}} y_{23} + 4m_{\text{KK}} y_{32}} - \frac{v_{H4}^2 y_{13}^2}{4m_{\text{KK}}^2} \\ -\frac{v_{H4} y_{13}}{\sqrt{2}m_{\text{KK}}} + \frac{v_{H4}^2 y_{13}(y_{23}+3y_{32})}{4\sqrt{2}m_{\text{KK}}^2} & \frac{v_{H4}(y_{21}^2-y_{13}^2)}{4m_{\text{KK}}(y_{23}+y_{32})} - \frac{v_{H4}^2 y_{13}^2}{4m_{\text{KK}}^2} & 1 - \frac{v_{H4}^2 y_{13}^2}{4m_{\text{KK}}^2} \end{pmatrix} \\ U'_R &\approx \begin{pmatrix} 1 - \frac{v_{H4}^2 y_{21}^2}{2m_{\text{KK}}^2} & -\frac{v_{H4} y_{21}}{\sqrt{2}m_{\text{KK}}} - \frac{v_{H4}^2 y_{21}(y_{23}+3y_{32})}{4\sqrt{2}m_{\text{KK}}^2} & \frac{v_{H4} y_{21}}{\sqrt{2}m_{\text{KK}}} - \frac{v_{H4}^2 y_{21}(y_{23}+3y_{32})}{4\sqrt{2}m_{\text{KK}}^2} \\ \frac{v_{H4} y_{21}}{\sqrt{2}m_{\text{KK}}} + \frac{v_{H4}^2 y_{21}(y_{23}+3y_{32})}{4\sqrt{2}m_{\text{KK}}^2} & 1 - \frac{v_{H4}^2 y_{21}^2}{4m_{\text{KK}}^2} & \frac{v_{H4}(y_{13}^2-y_{21}^2)}{4m_{\text{KK}} y_{23} + 4m_{\text{KK}} y_{32}} + \frac{v_{H4}^2 y_{21}^2}{4m_{\text{KK}}^2} \\ -\frac{v_{H4} y_{21}}{\sqrt{2}m_{\text{KK}}} + \frac{v_{H4}^2 y_{21}(y_{23}+3y_{32})}{4\sqrt{2}m_{\text{KK}}^2} & \frac{v_{H4}(y_{21}^2-y_{13}^2)}{4m_{\text{KK}}(y_{23}+y_{32})} + \frac{v_{H4}^2 y_{21}^2}{4m_{\text{KK}}^2} & 1 - \frac{v_{H4}^2 y_{21}^2}{4m_{\text{KK}}^2} \end{pmatrix}. \end{aligned} \quad (85)$$

Expanding the couplings to first order in v_{H4}/m_{KK} and to second order in $F(1 \mp 2c_{L,E})$ we get:

$$\begin{aligned} \tilde{y} &\approx \begin{pmatrix} y_{11} & \frac{y_{13} - v_{H4}y_{13}(y_{23}-5y_{32})}{\sqrt{2}} & \frac{v_{H4}(y_{23}-5y_{32})y_{13} + y_{13}}{4\sqrt{2}m_{KK}} \\ -\frac{y_{21}}{\sqrt{2}} + \frac{v_{H4}y_{21}(y_{23}-5y_{32})}{4\sqrt{2}m_{KK}} & -\frac{y_{23}+y_{32}}{2} + v_{H4} \left(\frac{(y_{23}-y_{32})^2}{4m_{KK}} + \frac{y_{13}^2+y_{21}^2}{2m_{KK}} \right) & \frac{y_{32}-y_{23}}{2} + \frac{v_{H4}(y_{13}-y_{21})(y_{13}+y_{21})}{4m_{KK}} \\ \frac{y_{21}}{\sqrt{2}} + \frac{v_{H4}(y_{23}-5y_{32})y_{21}}{4\sqrt{2}m_{KK}} & \frac{y_{23}-y_{32}}{2} + \frac{v_{H4}(y_{13}^2-y_{21}^2)}{4m_{KK}} & \frac{y_{23}+y_{32}}{2} + v_{H4} \left(\frac{(y_{23}-y_{32})^2}{4m_{KK}} + \frac{y_{13}^2+y_{21}^2}{2m_{KK}} \right) \end{pmatrix}, \\ \tilde{g}_L &\approx \begin{pmatrix} g_{L,11} & \dots & \dots \\ -\frac{g_{L,12}}{\sqrt{2}} + v_{H4} \left(\frac{(y_{23}-y_{32})g_{L,12}}{4\sqrt{2}m_{KK}} + \frac{(y_{21}^2-y_{13}^2)g_{L,12}}{4\sqrt{2}m_{KK}(y_{23}+y_{32})} + \frac{y_{13}(g_{L,11}-g_{L,33})}{\sqrt{2}m_{KK}} \right) & \dots & \dots \\ \frac{g_{L,12}}{\sqrt{2}} + v_{H4} \left(\frac{(y_{23}-y_{32})g_{L,12}}{4\sqrt{2}m_{KK}} + \frac{(y_{21}^2-y_{13}^2)g_{L,12}}{4\sqrt{2}m_{KK}(y_{23}+y_{32})} + \frac{y_{13}(g_{L,11}-g_{L,33})}{\sqrt{2}m_{KK}} \right) & \dots & \dots \end{pmatrix}, \\ \tilde{g}_R &\approx \begin{pmatrix} g_{R,11} & \dots & \dots \\ \frac{g_{R,13}}{\sqrt{2}} + v_{H4} \left(\frac{(y_{32}-y_{23})g_{R,13}}{4\sqrt{2}m_{KK}} + \frac{(y_{21}^2-y_{13}^2)g_{R,13}}{4\sqrt{2}m_{KK}(y_{23}+y_{32})} + \frac{y_{21}(g_{R,22}-g_{R,11})}{\sqrt{2}m_{KK}} \right) & \dots & \dots \\ \frac{g_{R,13}}{\sqrt{2}} + v_{H4} \left(\frac{(y_{23}-y_{32})g_{R,13}}{4\sqrt{2}m_{KK}} + \frac{(y_{13}-y_{21})(y_{13}+y_{21})g_{R,13}}{4\sqrt{2}m_{KK}(y_{23}+y_{32})} + \frac{y_{21}(g_{R,11}-g_{R,22})}{\sqrt{2}m_{KK}} \right) & \dots & \dots \end{pmatrix}, \end{aligned} \quad (86)$$

where for $\tilde{g}_{L,R}$, that are symmetric, we show only the first column, that involves the lightest state. The couplings between KK states are not shown since they are not needed in this article and they involve rather long expressions.

Using these results it is straightforward to compute the coefficients of dipole (42) and vector (44) operators, obtaining Eq. (45).

When flavor is taken into account, the couplings and the KK masses become 3×3 matrices, with $g_{L,jk}$ and $g_{R,jk}$, as well as m_{KK} being diagonal, whereas the Yukawa couplings y_{jk} have a non-trivial structure, Eq. (23). As an example, the second term of \tilde{m}_1 in Eq. (84) can be written as:

$$[v_{H4}^3 y_{13} (m_1^E)^{-1} y_{32} (m_1^L)^{-1} y_{21}]^{jk}, \quad (87)$$

with j, k being generation indices.

Finally, to go to the mass basis one has to perform a bi-unitary transformation in generation space. As described in sec. 4.2, we consider the limit where the masses of the would be 0-modes are approximated by the leading order term in powers of v_{H4}/m_{KK} and $F(1 \mp 2c)$, as in Eq. (28).

Below we consider the diagonalization in flavor space of the mass matrix of the charged leptons of the SM for BM1. We express the factors $\delta^{\alpha_E^{jk}}$ and $F(1 \mp 2c_{L,E}^j)$ in terms of powers of λ_C using Eqs. (26) and (29):

$$m_E \approx \frac{g_5}{\sqrt{L}} v_{H4} \begin{pmatrix} x_E^{11} \lambda_C^9 & x_E^{12} \lambda_C^{10} & x_E^{13} \lambda_C^{12} \\ x_E^{21} \lambda_C^9 & x_E^{22} \lambda_C^6 & x_E^{23} \lambda_C^8 \\ x_E^{31} \lambda_C^9 & x_E^{32} \lambda_C^6 & x_E^{33} \lambda_C^4 \end{pmatrix}. \quad (88)$$

The eigenvalues, that reproduce the masses of the charged leptons of the SM, are given to leading order by:

$$m_i = \frac{g_5}{\sqrt{L}} v_{H4} x_E^{ii} \lambda_C^{\omega_i}, \quad \omega_i = 9, 6, 4, \quad \text{for } i = 1, 2, 3, \quad (89)$$

and the Left- and Right-handed rotation matrices are:

$$U_{e_L} \approx \begin{pmatrix} 1 & \frac{x_E^{12}}{x_E^{22}} \lambda_C^4 & \frac{x_E^{12}x_E^{32}+x_E^{13}x_E^{33}}{(x_E^{33})^2} \lambda_C^8 \\ -\frac{x_E^{12}}{x_E^{22}} \lambda_C^4 & 1 & \frac{x_E^{22}x_E^{32}+x_E^{23}x_E^{33}}{(x_E^{33})^2} \lambda_C^4 \\ \frac{-x_E^{13}x_E^{22}+x_E^{12}x_E^{23}}{x_E^{22}x_E^{33}} \lambda_C^8 & -\frac{x_E^{22}x_E^{32}+x_E^{23}x_E^{33}}{(x_E^{33})^2} \lambda_C^4 & 1 \end{pmatrix},$$

$$U_{e_R} \approx \begin{pmatrix} 1 & \frac{x_E^{21}}{x_E^{22}} \lambda_C^3 & \frac{x_E^{31}}{x_E^{33}} \lambda_C^5 \\ -\frac{x_E^{21}}{x_E^{22}} \lambda_C^3 & 1 & \frac{x_E^{22}}{x_E^{33}} \lambda_C^2 \\ \frac{-x_E^{31}x_E^{22}+x_E^{21}x_E^{32}}{x_E^{22}x_E^{33}} \lambda_C^5 & -\frac{x_E^{32}}{x_E^{33}} \lambda_C^2 & 1 \end{pmatrix}, \quad (90)$$

where to simplify the expressions we have assumed real coefficients.

Armed with these matrices one can obtain the Wilson coefficients of sec. 5. In our calculations of the Wilson coefficients we have used expressions that contain higher orders in the expansion in powers of λ_C .

References

- [1] E. Witten, *Dynamical Breaking of Supersymmetry*, *Nucl. Phys. B* **188** (1981) 513.
- [2] S. P. Martin, *A Supersymmetry primer*, *Adv. Ser. Direct. High Energy Phys.* **18** (1998) 1–98, [[hep-ph/9709356](#)].
- [3] D. B. Kaplan and H. Georgi, *SU(2) x U(1) Breaking by Vacuum Misalignment*, *Phys. Lett. B* **136** (1984) 183–186.
- [4] D. B. Kaplan, H. Georgi and S. Dimopoulos, *Composite Higgs Scalars*, *Phys. Lett. B* **136** (1984) 187–190.
- [5] G. Isidori, Y. Nir and G. Perez, *Flavor Physics Constraints for Physics Beyond the Standard Model*, *Ann. Rev. Nucl. Part. Sci.* **60** (2010) 355, [[1002.0900](#)].
- [6] D. B. Kaplan, *Flavor at SSC energies: A New mechanism for dynamically generated fermion masses*, *Nucl. Phys. B* **365** (1991) 259–278.
- [7] Y. Grossman and M. Neubert, *Neutrino masses and mixings in nonfactorizable geometry*, *Phys. Lett. B* **474** (2000) 361–371, [[hep-ph/9912408](#)].
- [8] S. J. Huber and Q. Shafi, *Fermion masses, mixings and proton decay in a Randall-Sundrum model*, *Phys. Lett. B* **498** (2001) 256–262, [[hep-ph/0010195](#)].
- [9] T. Gherghetta and A. Pomarol, *Bulk fields and supersymmetry in a slice of AdS*, *Nucl. Phys. B* **586** (2000) 141–162, [[hep-ph/0003129](#)].
- [10] C. Csaki, C. Delaunay, C. Grojean and Y. Grossman, *A Model of Lepton Masses from a Warped Extra Dimension*, *JHEP* **10** (2008) 055, [[0806.0356](#)].

- [11] S. L. Glashow, J. Iliopoulos and L. Maiani, *Weak Interactions with Lepton-Hadron Symmetry*, *Phys. Rev. D* **2** (1970) 1285–1292.
- [12] K. Agashe, G. Perez and A. Soni, *Flavor structure of warped extra dimension models*, *Phys. Rev. D* **71** (2005) 016002, [[hep-ph/0408134](#)].
- [13] R. Contino, T. Kramer, M. Son and R. Sundrum, *Warped/composite phenomenology simplified*, *JHEP* **05** (2007) 074, [[hep-ph/0612180](#)].
- [14] G. F. Giudice, C. Grojean, A. Pomarol and R. Rattazzi, *The Strongly-Interacting Light Higgs*, *JHEP* **06** (2007) 045, [[hep-ph/0703164](#)].
- [15] C. Csaki, A. Falkowski and A. Weiler, *The Flavor of the Composite Pseudo-Goldstone Higgs*, *JHEP* **09** (2008) 008, [[0804.1954](#)].
- [16] A. Glioti, R. Rattazzi, L. Ricci and L. Vecchi, *Exploring the flavor symmetry landscape*, *SciPost Phys.* **18** (2025) 201, [[2402.09503](#)].
- [17] A. Davidson, M. Koca and K. C. Wali, *$U(1)$ as the Minimal Horizontal Gauge Symmetry*, *Phys. Rev. Lett.* **43** (1979) 92.
- [18] A. Davidson, V. P. Nair and K. C. Wali, *Peccei-Quinn Symmetry as Flavor Symmetry and Grand Unification*, *Phys. Rev. D* **29** (1984) 1504.
- [19] Y. Grossman, Y. Nir and Y. Shadmi, *Large mixing and large hierarchy between neutrinos with Abelian flavor symmetries*, *JHEP* **10** (1998) 007, [[hep-ph/9808355](#)].
- [20] C. D. Froggatt and H. B. Nielsen, *Hierarchy of Quark Masses, Cabibbo Angles and CP Violation*, *Nucl. Phys. B* **147** (1979) 277–298.
- [21] M. Leurer, Y. Nir and N. Seiberg, *Mass matrix models*, *Nucl. Phys. B* **398** (1993) 319–342, [[hep-ph/9212278](#)].
- [22] M. Leurer, Y. Nir and N. Seiberg, *Mass matrix models: The Sequel*, *Nucl. Phys. B* **420** (1994) 468–504, [[hep-ph/9310320](#)].
- [23] S. F. King, *Large mixing angle MSW and atmospheric neutrinos from single right-handed neutrino dominance and $U(1)$ family symmetry*, *Nucl. Phys. B* **576** (2000) 85–105, [[hep-ph/9912492](#)].
- [24] N. Haba and H. Murayama, *Anarchy and hierarchy*, *Phys. Rev. D* **63** (2001) 053010, [[hep-ph/0009174](#)].
- [25] D. Suematsu, *The Origin of quark and lepton mixings*, *Phys. Rev. D* **64** (2001) 073013, [[hep-ph/0104187](#)].
- [26] H. K. Dreiner and M. Thormeier, *Supersymmetric Froggatt-Nielsen models with baryon and lepton number violation*, *Phys. Rev. D* **69** (2004) 053002, [[hep-ph/0305270](#)].

[27] Y. Nir and Y. Shadmi, *The Importance of being majorana: Neutrinos versus charged fermions in flavor models*, *JHEP* **11** (2004) 055, [[hep-ph/0404113](#)].

[28] H. Kamikado, T. Shindou and E. Takasugi, *Froggatt-Nielsen hierarchy and the neutrino mass matrix*, [0805.1338](#).

[29] F. Plentinger, G. Seidl and W. Winter, *Group Space Scan of Flavor Symmetries for Nearly Tribimaximal Lepton Mixing*, *JHEP* **04** (2008) 077, [[0802.1718](#)].

[30] W. Buchmuller, V. Domcke and K. Schmitz, *Predicting θ_{13} and the Neutrino Mass Scale from Quark Lepton Mass Hierarchies*, *JHEP* **03** (2012) 008, [[1111.3872](#)].

[31] S. Krippendorf, S. Schafer-Nameki and J.-M. Wong, *Froggatt-Nielsen meets Mordell-Weil: A Phenomenological Survey of Global F-theory GUTs with $U(1)$ s*, *JHEP* **11** (2015) 008, [[1507.05961](#)].

[32] M. Bauer, T. Schell and T. Plehn, *Hunting the Flavon*, *Phys. Rev. D* **94** (2016) 056003, [[1603.06950](#)].

[33] Y. Ema, K. Hamaguchi, T. Moroi and K. Nakayama, *Flaxion: a minimal extension to solve puzzles in the standard model*, *JHEP* **01** (2017) 096, [[1612.05492](#)].

[34] K. Nishiwaki, Y. Shimizu and Y. Tatsuta, *Double Froggatt–Nielsen mechanism*, *PTEP* **2016** (2016) 083B05, [[1602.00890](#)].

[35] F. Feruglio and A. Romanino, *Lepton flavor symmetries*, *Rev. Mod. Phys.* **93** (2021) 015007, [[1912.06028](#)].

[36] M. S. Berger and M. Dawid, *A Froggatt–Nielsen flavor model for neutrino physics*, *Int. J. Mod. Phys. A* **34** (2019) 1950102, [[1901.10504](#)].

[37] A. Smolkovič, M. Tammaro and J. Zupan, *Anomaly free Froggatt–Nielsen models of flavor*, *JHEP* **10** (2019) 188, [[1907.10063](#)]. [Erratum: *JHEP* 02, 033 (2022)].

[38] S. Nishimura, C. Miyao and H. Otsuka, *Exploring the flavor structure of quarks and leptons with reinforcement learning*, *JHEP* **23** (2020) 021, [[2304.14176](#)].

[39] Y.-C. Qiu, J.-W. Wang and T. T. Yanagida, *Predictions of mee and neutrino mass from a consistent Froggatt–Nielsen model*, *Phys. Rev. D* **108** (2023) 115021, [[2307.16470](#)].

[40] J. Sato and K. Tobe, *Neutrino masses and lepton flavor violation in supersymmetric models with lopsided Froggatt–Nielsen charges*, *Phys. Rev. D* **63** (2001) 116010, [[hep-ph/0012333](#)].

[41] M. Bordone, O. Catà and T. Feldmann, *Effective Theory Approach to New Physics with Flavour: General Framework and a Leptoquark Example*, *JHEP* **01** (2020) 067, [[1910.02641](#)].

[42] P. Asadi, A. Bhattacharya, K. Fraser, S. Homiller and A. Parikh, *Wrinkles in the Froggatt-Nielsen mechanism and flavorful new physics*, *JHEP* **10** (2023) 069, [2308.01340].

[43] G. Pathak and M. K. Das, *Froggatt-Nielsen like mechanism in the framework of Modular Symmetry for Neutrino Mass, Mixing and Leptogenesis*, 2508.13578.

[44] T. Alanne, S. Blasi and F. Goertz, *Common source for scalars: Flavored axion-Higgs unification*, *Phys. Rev. D* **99** (2019) 015028, [1807.10156].

[45] M. Ibe, S. Shirai and K. Watanabe, *Comprehensive Bayesian exploration of Froggatt-Nielsen mechanism*, *JHEP* **03** (2025) 150, [2412.19484].

[46] C. Cornellà, D. Curtin, G. Krnjaic and M. Mellors, *Testing the Froggatt-Nielsen Mechanism with Lepton Violation*, 2501.00629.

[47] L. Calibbi, F. Goertz, D. Redigolo, R. Ziegler and J. Zupan, *Minimal axion model from flavor*, *Phys. Rev. D* **95** (2017) 095009, [1612.08040].

[48] L. Da Rold and F. Lamagna, *Composite Froggatt-Nielsen model of flavor*, *Phys. Rev. D* **105** (2022) 115020, [2112.14600].

[49] K. Agashe, A. E. Blechman and F. Petriello, *Probing the Randall-Sundrum geometric origin of flavor with lepton flavor violation*, *Phys. Rev. D* **74** (2006) 053011, [hep-ph/0606021].

[50] M. Beneke, P. Moch and J. Rohrwild, *Lepton flavour violation in RS models with a brane- or nearly brane-localized Higgs*, *Nucl. Phys. B* **906** (2016) 561–614, [1508.01705].

[51] L. Randall and R. Sundrum, *A Large mass hierarchy from a small extra dimension*, *Phys. Rev. Lett.* **83** (1999) 3370–3373, [hep-ph/9905221].

[52] S. Antusch and V. Maurer, *Running quark and lepton parameters at various scales*, *JHEP* **11** (2013) 115, [1306.6879].

[53] M. Hirsch and S. F. King, *Discriminating neutrino seesaw models*, *Phys. Lett. B* **516** (2001) 103–110, [hep-ph/0102103].

[54] T. Gherghetta, V. V. Khoze, A. Pomarol and Y. Shirman, *The Axion Mass from 5D Small Instantons*, *JHEP* **03** (2020) 063, [2001.05610].

[55] G. Cacciapaglia, C. Csaki, G. Marandella and J. Terning, *The Gaugephobic Higgs*, *JHEP* **02** (2007) 036, [hep-ph/0611358].

[56] G. Panico and A. Wulzer, *The Composite Nambu-Goldstone Higgs*, vol. 913. Springer, 2016, 10.1007/978-3-319-22617-0.

[57] F. Goertz, *Flavour observables and composite dynamics: leptons*, *Eur. Phys. J. ST* **231** (2022) 1287–1298.

- [58] F. Goertz, *Lepton Flavor in Composite Higgs Models*, *PoS PANIC2021* (2022) 149, [2112.01450].
- [59] F. Feruglio, P. Paradisi and A. Pattori, *Lepton Flavour Violation in Composite Higgs Models*, *Eur. Phys. J. C* **75** (2015) 579, [1509.03241].
- [60] ACME collaboration, J. Baron et al., *Order of Magnitude Smaller Limit on the Electric Dipole Moment of the Electron*, *Science* **343** (2014) 269–272, [1310.7534].
- [61] W. B. Cairncross, D. N. Gresh, M. Grau, K. C. Cossel, T. S. Roussy, Y. Ni et al., *Precision Measurement of the Electron’s Electric Dipole Moment Using Trapped Molecular Ions*, *Phys. Rev. Lett.* **119** (2017) 153001, [1704.07928].
- [62] ACME collaboration, V. Andreev et al., *Improved limit on the electric dipole moment of the electron*, *Nature* **562** (2018) 355–360.
- [63] T. S. Roussy et al., *An improved bound on the electron’s electric dipole moment*, *Science* **381** (2023) adg4084, [2212.11841].
- [64] PARTICLE DATA GROUP collaboration, S. Navas et al., *Review of particle physics*, *Phys. Rev. D* **110** (2024) 030001.